Atmospheric methane evolution the last 40 years

S. B. Dalsøren[1], C. L. Myhre[2], G. Myhre[1], A. J. Gomez-Pelaez[3], O. A. Søvde[1], I. S. A. Isaksen[1,4], R. F. Weiss[5], C. M. Harth[5]

[1]CICERO - Center for International Climate and Environmental Research Oslo, Oslo, Norway

[2]NILU - Norwegian Institute for Air Research, Kjeller, Norway

[3]Izaña Atmospheric Research Center (IARC), Meteorological State Agency of Spain (AEMET), Izaña, Spain

[4] University of Oslo, Department of Geosciences, Oslo, Norway

[5]Scripps Institution of Oceanography University of California, San Diego La Jolla, California, USA

Correspondence to: S. B. Dalsøren (stigbd@cicero.oslo.no)

Abstract

Observations at surface sites show an increase in global mean surface methane (CH_4) of about 180 parts per billion (ppb) (above 10 %) over the period 1984-2012. Over this period there are large fluctuations in the annual growth rate. In this work, we investigate the atmospheric CH_4 evolution over the period 1970-2012 with the Oslo CTM3 global Chemical Transport Model (CTM) in a bottom-up approach. We thoroughly assess data from surface measurement sites in international networks and select a subset suited for comparisons with the output from the CTM**.** We compare model results and observations to understand causes for both long-term trends and short-term variations. Employing Oslo CTM3 we are able to reproduce the seasonal and year to year variations and shifts between years with consecutive growth and stagnation, both at global and regional scales. The overall CH_4 trend over the period is reproduced, but for some periods the model fails to reproduce the strength of the growth. The model overestimates the observed growth after 2006 in all regions. This seems to be explained by a too strong increase in anthropogenic emissions in Asia, having global impact. Our findings confirm other studies questioning the timing or strength of the emission changes in Asia in the EDGAR v4.2 emission inventory over the last decades. The evolution of CH_4 is not only controlled by changes in sources, but also by changes in the chemical loss in the atmosphere and soil uptake. The atmospheric CH_4 lifetime is an indicator of the CH_4 loss. In our simulations, the atmospheric CH_4 lifetime decreases by more than 8 % from 1970 to 2012, a significant reduction of the residence time of this important greenhouse gas. Changes in CO and NO_x emissions, specific humidity, and ozone column drive most of this, and we provide simple prognostic equations for the relations between those and the CH_4 lifetime. The reduced lifetime results in substantial growth in the chemical CH_4 loss (relative to its burden) and dampens the CH_4 growth.

1 Introduction

The atmospheric CH_4 abundance has more than doubled over the industrial era. The resulting radiative forcing is second after CO_2 in terms of anthropogenic forcing from greenhouse gases (Myhre et al., 2013). High uncertainty remains regarding the contributions from specific source sectors and regions to the CH_4 emissions (Neef et al., 2010;Kirschke et al., 2013;Houweling et al., 2014;Melton et al., 2012;Bruhwiler et al., 2014;Schwietzke et al., 2014;Bridgham et al., 2013;Pison et al., 2009;Ciais et al., 2013), the underlying factors

contributing to observed trends (Dlugokencky et al., 2009;Dlugokencky et al., 2003;Wang et al., 2004;Kai et al., 2011;Aydin et al., 2011;Simpson et al., 2012;Bousquet et al., 2006;Bousquet et al., 2011;Pison et al., 2013;Bergamaschi et al., 2013;Monteil et al., 2011;Ghosh et al., 2015;Nisbet et al., 2014;Fiore et al., 2006;Levin et al., 2012), and in feedbacks from the biosphere and permafrost (Bridgham et al., 2013;Melton et al., 2012;Isaksen et al., 2011;O'Connor et al., 2010). The uncertainties in our understanding of current budgets, recent trends, and feedbacks limit confidence in accurately projecting the future evolution of CH_4. Increasing atmospheric CH_4 would accelerate near-term warming, due to its strong climate impact on a 20-year time frame (Myhre et al., 2013). Enhanced CH_4 levels would also increase the ozone levels in surface air (Fiore et al., 2008;West and Fiore, 2005;Fiore et al., 2012;Isaksen et al., 2014), and thereby worsen air pollution impacts on vegetation, crops, and human health.

This study seeks to increase our understanding of CH_4 by providing a detailed analysis on global and regional CH_4 evolution over the last 40 years. We investigate essential natural and anthropogenic drivers controlling the atmospheric CH_4 budget over the period, with a particular focus on the last 15 years. We perform a balanced analysis of both sources and sinks. The sinks depend on the atmospheric oxidation capacity, which is determined by complex chemical and meteorological interactions. This study tries to reveal the key chemical components and meteorological factors affecting recent changes in the oxidation capacity. We compare model studies and observations to understand causes for both long-term trends and short-term variations (year-to-year). We also address reasons for differences between observed and modelled CH_4 trends. The methods used are described in section 2. Section 3 presents the results from our main analysis and discuss them in a broader context related to findings from other studies. Additional sensitivity studies are presented in the Supplement. In section 4 we summarize our findings.

2 Methods and approach

2.1 Emissions and sinks

2.1.1 Methane

We used CH_4 emissions for anthropogenic sources from EDGAR v4.2 (EC-JRC/PBL, 2011) and biomass burning and natural sources from Bousquet et al. (2011). In addition we used soil uptake from Bousquet et al. (2011). Combination of two emission inventories (EDGAR v4.2

and Bousquet et al. (2011)) makes it possible to study the impacts of many emission sectors (18 in total, see Table S1 in the Supplement for the sectors and specifications of the categories). The EDGAR inventory covers the period 1970-2008 while the Bousquet et al. (2011) data covers the period 1984-2009. Since we study the period 1970-2012 extrapolations were made for the years not covered by the datasets. For all years from 1970 to 1984 we used natural and biomass burning emissions and soil uptake for 1984. For 2010-2012 we used 2009 data for these sources. For the anthropogenic emissions we extrapolated the change from 2007-2008 to the period 2009-2012. The rather simple extrapolations result in additional uncertainties in the model outcome for these years. Fig. S1 in the Supplement shows how the emissions are included in the model for the different time periods. The total emissions and emissions from major sectors are shown in Fig. 1. There is a large growth in total emissions from 1970 to 2012. However, shorter periods with declining emissions occur due to large inter-annual variability in natural emissions, especially from wetlands which is the largest emission sector. The inter-annual variation in wetland emissions tends to be anti-correlated with the ENSO index (Bousquet et al., 2006;Hodson et al., 2011). Low natural emissions also occur due to lower global temperatures in the years after the Pinatubo eruption. In the 1990s the growth in anthropogenic emissions are small, mainly caused by the economic collapse of the former USSR. From 2000 to 2006 the total emissions are quite stable and this is caused by decreasing wetland emissions due to dry conditions in the tropics in combination with increasing anthropogenic emissions. From 2006 there is a strong growth in total emissions due to large wetland emissions and a continuing growth of anthropogenic emissions. The abrupt increase in 2007 is mainly explained by high wetland emissions caused by high temperatures at high latitudes in the Northern Hemisphere, and wet conditions in the tropics (Bousquet et al., 2011). Enteric fermentation (due to ruminants) is the main anthropogenic emission sector and it grows steadily except for a period in the nineties. Some other major anthropogenic sectors like gas, solid fuel (mostly coal) and agricultural soils (mostly rice) even decrease over shorter periods but have in common a substantial growth over the last decade. The sum of several smaller anthropogenic emission sectors (industry, residential, waste, some fossil, etc.) are also shown in Fig. 1. This sum termed “other anthropogenic sectors” is of the same magnitude as enteric fermentation. The growth is rather stable and moderate with some interruptions: Temporary declines occur after the oil crisis in 1973 and the energy crisis in 1979. The growth is also small during the nineties.

We also explore a possible impact of the recent financial crisis using an alternative extrapolation of anthropogenic emissions for the period 2009-2012. Here, the emissions from petroleum and solid fuel production and distribution were scaled with BP Statistical Review of World Energy (bp.com/statisticalreview) numbers for gas production, oil and coal consumption resulting in a drop in total emissions in 2009 (Fig. 1). However, the evolution from 2010 with this alternative extrapolation is rather similar to that for the standard extrapolation. The EDGAR v4.2 inventory was recently extended to include also the years 2009-2012. In Figure S2 (supplement) we compare our extrapolations with the new data and also include a comparison to ECLIPSE v5a emissions that are available for part of our study period (1990-2015, 5-year intervals).

2.1.2 Other components

Anthropogenic emissions of CO, NOx, sulfur and NMVOCs were taken from the EDGAR v4.2 inventory (EC-JRC/PBL, 2011). Similar extrapolation was done as for the CH_4 emissions to cover the period 2009-2012. For biomass burning emissions we used GFEDv3 (van der Werf et al., 2010) for the period 1997-2012. In the period 1970-1996 we used year 2001 emissions from GFEDv3. 2001 was taken as a proxy for an average year since it has a weak ENSO index for all months (see next section for more discussion on this).

The parametrization and inter-annual variation of lightning NO_x emissions are described in Søvde et al. (2012). For other natural emissions we used emission data for 2000 for all years. The oceanic emissions of CO and NMVOCs and soil NOx emissions are from RETRO (Schultz et al., 2008). Sources for natural sulfur emissions are described in Berglen et al. (2004). The emissions from vegetation of CO and NMVOCs are from MEGANv2 (Guenther et al., 2006). Recently a new dataset (Sindelarova et al., 2014) with MEGAN emissions covering the period 1980-2010 became available. This dataset was used in a sensitivity study to investigate whether inter-annual variations in CO and NMVOCs emissions from vegetation are important for the CH_4 evolution.

2.2 Chemical Transport Model

The emission data over the period 1970-2012 was used as input in the Oslo CTM3 model. A coupled tropospheric and stratospheric version was used. The model was run with 109 chemical active species affecting CH_4 and atmospheric oxidation capacity. In addition we added 18 passive fictitious tracers for each of the CH_4 emission sectors listed in Table S1. The

traces were continuously emitted and then given an e-folding lifetime of 1 month undergoing transport but not interacting chemically. The passive tracers were used as a proxy for the different sector's contribution to monthly mean surface CH_4 concentrations. The aim was to reveal key sectors and regions behind recent changes in spatial distribution or temporal evolution of CH_4.

Oslo CTM3 was described and evaluated by Søvde et al. (2012) and used for studying CH_4 lifetime changes in Holmes et al. (2013). Oslo CTM3 is an update of Oslo CTM2 which has been used in a number of previous studies of stratospheric and tropospheric chemistry, including studies on CH_4 (Dalsoren et al., 2010;Dalsøren and Isaksen, 2006;Dalsøren et al., 2011;Isaksen et al., 2011).

The Oslo CTM3 simulations were driven with 3-hourly meteorological forecast data from the European Centre for Medium-Range Weather Forecasts (ECMWF) Integrated Forecast System (IFS) model (see Søvde et al. (2012) for details). These data are 36-hours forecasts produced with 12 hours of spin-up starting from an ERA-Interim analysis at noon on the previous day. The meteorological data used in this study cover the period 1997-October 2012. For the years ahead of 1997, year 2001 meteorology was used. 2001 was chosen since this is a year with weak ENSO index for all months. Previous studies have shown a strong influence of ENSO events on CH_4 (Holmes et al., 2013;Warwick et al., 2002;Johnson et al., 2002). Initially the model was spun up in a long run with repetitive 1970 emissions until we obtained a stable atmospheric CH_4 burden from one year to the next. Due to the long adjustment time of CH_4 it took 27 years to get CH_4 in equilibrium. After the spin up a set of simulations (Table 1) were made for the period 1970 to 2012. The «main» simulation includes the standard CH_4 emissions described in section 2.1.1. In the «financial» simulation the period 2009-2012 was rerun with slightly different emissions evaluating whether the recent financial crisis had any significant impact on CH_4 levels. With a similar purpose a "bio" simulation was performed accounting for inter-annual variation in emissions of CO and NMVOCs from vegetation. The results from the two sensitivity studies on emissions are discussed in the Supplement. In the «fixed methane» simulation, the prescription of methane emissions was turned off and surface CH_4 was kept fixed at monthly mean 1970 levels (i.e., boundary condition of Dirichlet type instead of Neumann type) to isolate the effect of other components and meteorological factors on CH_4 *via* changes in oxidation capacity. In the «fixed met» simulation, the period 1997-2012 was repeated using year 2001 meteorology for all years. By comparing this run with the «main» simulation the impact of meteorological variability could be discerned.

2.3 Observations

To get insights into the drivers of the changes on regional level, and reveal strengths and discrepancies in model performance we compared the model results to surface CH_4 observations. We thoroughly assessed the surface sites providing CH_4 measurements to the World Data Center for Greenhouse Gases (WDCGG) (http://ds.data.jma.go.jp/gmd/wdcgg/), and picked out a subset of sites for comparison. Criteria for selection were the length of measurement record (coverage over most of the time periods of interest), access to continuous time series with few gaps, time resolution (at least 2-3 measurement per month), coverage of different regions of the Earth, and site characteristics (e.g. elevation, topography, and influence of pollution episodes). The last point was evaluated in relation to the resolution of the CTM. From this analysis, 71 observational datasets from 64 stations in the WDCGG database were selected as suited for comparisons with the CTM results. Comparisons for some of these stations are shown in sections 3.3 and 3.4.

3 The methane evolution and decisive factors over the period 1970-2012

3.1 Global methane budget

Fig. 2 shows the evolution of the CH_4 budget over the period 1970-2012 for the main simulation. It presents total burden and loss calculated by the forward CTM run and the emissions applied in this simulation. The total burden shown in black is balanced by the emissions (blue) and the loss (red). There is a steady growth in atmospheric CH_4 burden from 1970 to the beginning of the nineties, then a short period of decline after the Mount Pinatubo volcanic eruption in 1991. After 1994 there is a slight increase in CH_4 burden towards the millennium. Then the CH_4 burden is stable for 5-6 years. After 2006 there is a rapid growth in CH_4 burden.

The evolution of emissions and the modelled CH_4 burden share many common features (Fig. 2). However, the growth in emissions is about 35 % from 1970 to 2012 while the growth in atmospheric burden is about 15 % (additional burden increase after 2012 due to the long response time of CH_4, is not accounted for in this number). The CH_4 burden increased less than expected solely from the increase in CH_4 emissions since a growth in the atmospheric CH_4 loss occurred over the period. The growth in instantaneous atmospheric CH_4 loss is almost 25 %. In the period 2001-2006 when emissions were quite stable increasing CH_4 loss likely contributed to the stagnation of the CH_4 growth. Interestingly, for 2010-2012, the loss

deviates from its steady increase over the previous decades. A stabilization of the CH_4 loss probably contributed to the continuing increase (2009-2012) in CH_4 burden after the high emission years 2007 and 2008. Due to the long response time of CH_4 this change in the loss pattern might also contribute to future growth in CH_4. However, there are additional uncertainties in the model burden and loss after 2009 due to the extrapolation of emissions after this year.

Especially after 1997 and the introduction of variation in meteorology, we see that the loss follows a different path than the burden. Comparing the main model simulation with the one with fixed meteorology (Fig. 3) for the period 1997-2012 it becomes evident that inclusion of varying meteorological factors is important to take into account to understand the development of the CH_4 budget. This was also shown in other studies (Johnson et al., 2002;Fiore et al., 2006;Warwick et al., 2002;Holmes et al., 2013). If there had been no variation in meteorology and only changes in emissions, the CH_4 loss would have been significantly different and there would have been a stronger increase in CH_4 burden after 2006. Meteorological variability explains to a large degree much of the stabilization of CH_4 loss after 2010, and might thereby explain part of the large CH_4 burden increase in 2011 and 2012. Around the millennium we see a stabilization of the loss in the simulation with fixed meteorology, but increased loss in the main run. This implies that meteorological variations contribute to a prolonged period (2003-2006) of stabilization in CH_4 burden (Fig. 3). From the comparison in Fig. 3 it can also be seen that it is meteorological factors and not emissions that causes the large enhancements of CH_4 loss in 1998 (El Niño event) and 2010 (warm year on global scale). Such episodes do not show up as immediate perturbations of the CH_4 burden (Fig. 2 and 3) due to the long response time of atmospheric CH_4. Meteorology and other drivers for the modelled evolution of methane loss are discussed in detail in sections 3.5-3.6.

3.2 Evolution of global mean surface methane

Fig. 4 compares the global mean surface CH_4 in the main model simulation, to global mean surface CH_4 calculated from networks of surface stations. The main picture is discussed in this section while more detailed evaluations of CH_4 development on continental scale, trends, and inter-annual variations are made in the following sections. The time evolution of global mean surface CH_4 is very similar for the three observational networks shown in Fig. 4 but there are some differences for the absolute methane level. The AGAGE (mountain and coastal sites) and NOAA ESRL (sites in the marine boundary layer) stations are distant from large pollution sources. WDCGG uses curve fitting and data extension methods very similar to

those developed by NOAA and many of the same stations (Tsutsumi et al., 2009), but in addition to marine boundary layer sites, WDCGG includes many continental locations strongly influenced by local sources and sinks (**http://www.esrl.noaa.gov/gmd/ccgg/mbl/mbl.html**). The methane emission estimates from Bousquet et al. (2011) are optimized against atmospheric observations. Since we only use their natural and biomass burning emission inventories, we use different anthropogenic emissions (from EDGAR), and the OH field in their inverse model is substantially different from our modelled OH, there is no guarantee that our model will match observations.

Our model generally reproduces the different periods of growth and stagnation and the overall observed increase in concentration from 1984 to 2012 of almost 180 ppb is replicated. This gives us confidence when evaluating the decisive drivers explaining the variable evolution over time. However, the model fails to reproduce the strength of the growth rate during some eras, for instance the growth since 2006 is overestimated. Over the whole period the model also underestimate the observed CH_4 level. Even though there are also large uncertainties in total CH_4 emission levels (Kirschke et al., 2013;Ciais et al., 2013) we find it more likely that our model overestimates the atmospheric CH_4 sink. In a recent model inter-comparison the multi-model global mean CH_4 lifetime was underestimated by 5-13 % (Naik et al., 2013) compared to observational estimates. Our study shows a similar underestimation of CH_4 lifetime. Though the multi-model lifetime is within the uncertainty range of observations it is likely that models tend to overestimate OH abundances in the Northern Hemisphere (Naik et al., 2013;Strode et al., 2015;Patra et al., 2014).

3.3 Methane evolution and emission drivers in different regions

In the Supplement, we explain how the CH_4 mole fraction can be split into two components: A quite uniform background component and an inhomogeneous recently emitted component. The latter is advected and mixed, and when achieving a good mixing (after 1-2 months) it is converted into the background component. We show how the use of a 1-month e-folding fictitious tracer (Total tracer) is valid as a proxy for the inhomogeneous component. The CH_4 surface emissions act as the sources for the tracer. In the Supplement we use the continuity equation for the CH_4 mole fraction (CH_4 model) as starting point and further arguments to derive the following approximation:

$\langle CH_4 \text{ model} \rangle - [\langle CH_4 \text{ model} \rangle] = B \times (\langle \text{Total tracer} \rangle - [\langle \text{Total tracer} \rangle]) + \text{Residual}$ (Equation 1)

Where [ ] denotes longitudinal mean along a whole terrestrial parallel and < > denotes annual running mean. We are interested in the inter-annual variation of CH_4, so we have carried out annual running means to remove the strong seasonal cycle. The subtraction of longitudinal means on each side of Eq. 1 removes the influence of differences in lifetimes (the mean lifetime of CH_4 is around 9 years, whereas the mean lifetime of the Total tracer is 1 month). B and Residual are constants (or almost constant), if the prerequisites discussed in the Supplement (S3, last paragraph) are met. We expect B to be near or equal to 1, and Residual to be small. If B and Residual were exactly constant, the Pearson linear correlation coefficient between $\langle CH_4 \text{ model} \rangle - [\langle CH_4 \text{ model} \rangle]$ and $\langle \text{Total tracer} \rangle - [\langle \text{Total tracer} \rangle]$ would be exactly equal to 1. The tracer approach then gives valuable information on the contribution to CH_4 variation from recent regional-local emission or transport changes. We therefore use the correlation coefficient (indeed, its square, R^2: the coefficient of determination obtained when performing a linear least-square fit between both magnitudes in Eq. 1 to determine B and Residual) as one criterion when selecting interesting stations for methane trend studies. Only stations where R^2 is higher than 0.5 is used. This criterion excludes only a small number of the available stations. In addition, we use the general station selection criteria discussed earlier in the manuscript (sufficient coverage in the different world regions, long time series etc., see section 2.3). Fig. 5 shows the locations of stations used in Fig. 6-10 for detailed trend analysis and evaluation of model performance.

Table 2 shows R^2, the constants B and Residual, and RMSE from a linear fit of the variables in eq. 1. All stations except one (reason for exception at the Wendover station is discussed in the Supplement) have R^2 above 0.8. Such high coefficients support that the approximation in eq. 1 is useful for these stations. As expected, B is usually larger than 1. The fictitious tracer will underestimate somewhat the inhomogeneous recently emitted CH_4, in particular at remote stations, because part of it is removed by the e-folding sink before being smoothed to the characteristic variation length of the background. Mauna Loa is probably the most remote station and located at high altitude. It has the largest B and Residual. Alert, Tutuila, Mahe Island and Key Biscayne are also remote stations that have a high B. As explained below the tracers play a small role in explaining CH_4 at Cape Grim and Ushuaia, for which B is below 1.

In the upper panels of Fig. 6-10, the model results are scaled to the observed mean CH_4 level over the periods of measurements to better discern differences in trends between observations and model. The scaling procedure is explained in the Supplement. In general, the model reproduces the seasonal and year-to-year variations very well with high coefficients of determination, R^2, for most stations, (The median is 0.76, and R^2 is above 0.65 for 15 of 18 stations). The model performance is lower at highly polluted sites due to large gradients in concentrations and non-linearity of oxidant chemistry not fully captured by a global model with coarse resolution (approximately 2.8° x 2.8°). The model also captures the long term evolution of CH_4 seen in the observations but overestimates the increase after 2005 at most stations.

The stations in the Southern Hemisphere (Fig. 6) are located far from the dominating emissions sources, and the CH_4 concentration is to a large degree determined by transport and chemical loss. The high coefficients of determination ranging from 0.92 to 0.95 and reproduction of the seasonality and trends indicate that our model is performing excellent with respect to transport and seasonal variation in the chemical loss.

As seen in the mid panels, Ascension Island (Fig. 6a) and Tutuila (Fig. 6b) have negative <Total tracer>-[<Total tracer>]. Since these are rather remote stations, their tracer levels are below the longitudinal mean. The modelled CH_4 evolution from 1990-2005 is well correlated with the development of the natural tracers. However, changes in natural emissions do not seem to explain the periods with large growth before 1990 and for the period 2005-2012. While the model underestimates the growth before 1990 it overestimates the growth in the recent years. The small steady increases in contributions from all anthropogenic sectors only has a minor contribution to the modelled CH_4 increase for these periods. However, since these source tracers have an e-folding lifetime of 1 month their evolution is only representative for changes in contribution from regional sources. Inter-hemispheric transport occurs on longer timescales; hence, changes in large anthropogenic sources in the Northern Hemisphere most likely also had a significant contribution as discussed below. At Ascension Island, extra strong influences of regional sources (<CH_4 model>-[<CH_4 model>] change different from zero) are mainly associated with El Nino episodes (1987, 1997-98, and 2004-05). In 1997-98 there are peaks both for the natural tracer and <Total tracer>-[<Total tracer>] indicating a rise in nearby natural emissions and/or transport from such a source. For 1987 a regional drop in natural emissions has a smaller impact at Ascension compared to the whole latitude band. At Tutuila <Total tracer>-[<Total tracer>] decreases over time due to a relatively larger increase

in the latitudinal mean anthropogenic tracers (not shown), especially enteric fermentation. This explains why the CH_4 growth at the site (<CH_4 model>) is slightly less than the mean latitudinal ([<CH_4 model>]) growth.

Ushuaia (Fig. 6c) and Cape Grim (Fig. 6 d) are the southernmost stations. In the mid panels it can be seen that both terms on the right side in eq. 1 are small (B x (<Total tracer>-[<Total tracer>] and Residuals) resulting in small (<CH_4 model>-[<CH_4 model>]. This indicates that the contribution to CH_4 from regional emissions are small and that long-range transport from other latitudes is decisive. Distant latitudinal transport is not seen by the tracer term if it takes more than around two months. Such transport would also result in very similar <CH_4 model> and [<CH_4 model>] since atmospheric species with lifetime of that timescale or longer are quite homogenously distributed over latitudinal bands. Since both the emissions and their trends are small at high southern latitudes, the distant transport likely originates from low latitudes in the Southern Hemisphere or the Northern Hemisphere.

At stations in or near North America (Fig. 7) the model reproduces the observed trends with increases in the eighties, less change in the period 1990-2005 and increase from 2006. For the latest period the increase in the model is larger than that observed. The seasonal and year-to-year variations are well represented by the model at all stations (coefficients of determination from 0.73-0.82). Key Biscayne (Fig. 7c) and Mauna Loa (Fig. 7d) have relatively large negative <Total tracer> - [<Total tracer>] which shows that these are background stations and that important emission sources exist at their latitude. The tracer difference is quite small and negative at Alert (Fig. 7b) and since the Residual is quite close to zero this may indicate small sources at the station latitude. The contribution from natural emissions is decisive for year to year variations at all four stations in Fig. 7, and the influence of emission from the gas sector increases gradually. Key Biscayne situated in the boundary layer (Fig. 7c) is mostly influenced by emissions from the American continent, and the rest of the anthropogenic sectors have moderately declining impact after 1990. However, this decline occurs only initially for the solid fuel (mainly coal) sector as its contribution increases from 2003 and onwards. The same occurs for this sector at Alert (Fig. 7a). It corresponds with the start of an increase in U.S. fugitive solid fuel emissions in the applied EDGAR v4.2 inventory. The increase in U.S. coal emissions from 2003 to 2008 is almost 12 % in EDGAR v4.2. An increase of 28 % is found from 2005-2010 in the EPA inventory (EPA 2012). At the high

altitude sites Mauna Loa and Wendover (Fig. 7b and d) there are small or large increases in the contribution from all anthropogenic sectors from year 2000 and onwards. These stations are subject to efficient transport from Asia at high altitudes. There are large emission increases after 2000 in eastern Asia in the EDGAR v4.2 inventory (Bergamaschi et al., 2013). Especially coal related emissions in China show a strong increase with a doubling from 2000 to 2008.

At Wendover, Mauna Loa and Key Biscayne <Total tracer> - [<Total tracer>] decrease over the three decades studied (Fig. 7, mid panels). Several emission sectors contribute, The implication is a lower growth rate for <CH_4 model> than for [<CH_4 model>] (Fig. 7, mid panels), i.e. other locations (Asian stations, see discussion below) at the same latitudes have a larger trend in CH_4. There are large fluctuations of tracer transport to Mauna Loa in 1997-1998 and 2010-2011 that strongly impacts <CH_4 model> . The observations also show changes in growth and seasonal pattern these years.

At the Arctic site Zeppelin (Fig. 8a) located at the coast of West Svalbard there is a small CH_4 increase both in model and observations up to 2004. A large part of the CH_4 variability in the period 1997-1999 (Morimoto et al., 2006) was due to fluctuations in wetland and biomass burning emissions. Our modelled variation in the natural source tracer conforms to the fluctuations deduced from the isotopic measurements of Morimoto et al. (2006). Seasonal tracer analysis (not shown) is in agreement with the conclusion of Fisher et al. (2011), who found that wetlands are the main contributor in summer and gas in winter. A CH_4 concentration drop from 2004 to 2006 seems to mainly be explained by natural source contribution in the model falling from a period maximum in 2004 to low values in 2005-2006. This is also the case for the sub-Arctic site Pallas (Fig. 8b) located in a region characterised by forest and wetlands. Gas, enteric fermentation and various other small regional anthropogenic sources seems to contribute to the CH_4 increase at Zeppelin after 2006. The contribution from natural emissions and recent regional coal mining peaked in 2007. A quite strong CH_4 enhancement occurs for 2009-2010 in both the model and observations. The longitudinal mean tracers for individual sectors are almost stable to declining (not shown) while contribution from the <Gas> and some other tracers show a small maximum (Lower panel Fig. 8a and b). Pallas has a similar pattern. The runs with fixed meteorology suggest enhanced transport from Russia passing major gas fields and Pallas.

Mace Head (Fig. 8c) is a rural background coastal site in Europe. <Total tracer> - [<Total tracer>] is quite large and negative suggesting important emission sources along the station's latitude. In the beginning of the nineties, there is a mismatch between declining model concentrations and the increase found from the observations. Some of the decrease in the model is due to decreasing contributions from solid fuel (mainly coal), enteric fermentation and other regional anthropogenic sources. The station experiences unusual meteorological conditions in the ENSO year 1997, as there are abrupt shifts in concentrations of CH_4 and several of the anthropogenic tracers having small year-to-year variations in emissions. Similarly, there seems to be transport of less polluted air masses to the station in 2004 compared to earlier years resulting in lower CH_4 concentration in measurements and model in 2004 and 2005. Several regional sources seem to have small contributions to the modelled and observed CH_4 increases from 2006 to 2009. After 2009 we extrapolate emission trends due to lack of emission inventories and this may be the cause why the model doesn't reproduce the observed levelling off in growth in 2010 and 2011.

The model has larger discrepancies at Hegyhatsal, a semi-polluted site in central Europe (Fig. 8d). Despite seasonal issues the model performance is reasonable for the long term CH_4 changes. In years with high contributions from natural sources, the seasonal maxima tend to be too high in the model. It could be that the coarse model resolution results in too much transport from nearby wetlands or that the emission inventory has too large natural emissions in surrounding regions. <Total tracer> - [<Total tracer>] is very large and positive meaning that the station is very sensitive to emissions close upwind. The evolution of <CH_4 model> therefore deviates strongly from the longitudinal mean [<CH_4 model>]. The deviation starts in 1996 when a sharp increase in natural emission occurs. From 2003-2008 there is a period with stable to declining modelled CH_4 concentrations. This is caused by decreasing central European emissions particularly from enteric fermentation and the category "other anthropogenic sectors" together with decreasing or fluctuating natural sources.

In general, the model reproduces the features in the observations over and near Asia quite well (Fig. 9 and 10) with coefficient of determination in the range of 0.24-0.84. For the trends, the overestimation after year 2006 is higher here than modelled in other world regions (Fig. 6-8). Gas is the major cause of increases in CH_4 in Israel (Sede Boker, Fig. 9a). The increase of the <Gas> tracer is much larger than for the longitudinal mean [<Gas>] suggesting important emission increases from nearby gas fields. Small changes in regional natural emissions and the category other anthropogenic sources (lower panel) is correlated with the modelled year-

to-year variations (upper panel). The station in Kazakhstan (Fig. 9c) is downwind of large sources (<Total tracer> - [<Total tracer>] large and positive) and the modelled CH_4 increase after 2005 is much larger than for the longitudinal mean. Also at this station, the CH_4 trend is heavily influenced by gas, although not to the same extent as in Israel. Other regional anthropogenic emission changes also contribute somewhat to the modelled CH_4 increase over the last years. High natural emissions in 2008-2009 also had an impact. Since we use repetitive year 2009 natural emissions for the latter years it could be that the contribution from this source is too large after 2009. Unfortunately, the modelled CH_4 increase cannot be confirmed by measurements since data at the station is missing after 2008.

Regional solid fuel emissions (mainly coal) is the main cause of last decade modelled CH_4 increase in eastern continental Asia (Ulaan Uul and Tae-ahn Peninsula, Fig. 9b and d) but gas and other reginal anthropogenic sectors also contribute. There is large growth in <CH_4 model> for Ulaan Uul in 2006-2007 and 2010 mainly due to peaks in the contribution from solid fuel sources but also other anthropogenic sectors have a role in this. Similar pattern appears for Tae-ahn Peninsula in 2009. The first peak at Ulaan Uul is also partly seen in the observations, but the existence of the latest episode and the event at Tae-ahn Peninsula is less clear from the measurements. Our tracer analysis for Minamitorishima (not shown), a background station affected by outflow from the Asian continent indicates less continental outflow in 2007. For these polluted continental sites the correlation coefficients are lower than for the other stations. The coarse resolution of the model has problems resolving large gradients in concentrations and non-linearity of oxidant chemistry. At Tae-ahn Peninsula <CH_4 model> starts increasing in 2005 while the increase at Ulaan Uul first starts in 2006. At Ulaan Uul decreasing regional natural emissions over the period 2000-2005 seems to compensate for the large increase of solid fuel emissions from around 2000.

For Cape Rama in India (Fig 10a, the observations show signatures of both Northern and Southern Hemispheric (NH and SH) air masses (Bhattacharya et al., 2009). Mixed with regional fluxes and varying chemical loss this results in large seasonal variation. During the summer monsoon, the station is located south of the inter-tropical convergence zone. Air arriving during this period (June to September) represent tropical or SH oceanic air masses and the station is upwind of Mahe Island (Fig. 10b). During the winter monsoon the situation is opposite. There is outflow from the continent affecting both Cape Rama and Mahe Island. The ENSO event in 1997 seems to have opposite effects on modelled and observed CH_4 variability at Cape Rama. Except from that, the model does a reasonable job in reproducing

the measurements. Most regional tracers show stable to upward levels over the period of comparison and likely contribute to a small fraction of the modelled CH_4 trend. At Mahe Island in the SH (Fig. 10b), the CH_4 concentration peaks sharply during NH winter when the station is influenced by outflow from continental Asia. The station is therefore an indicator of inflow to the SH. This feature is well captured by the model. Over the last decade, there is a small and continuous rise in the levels of all anthropogenic tracers at the station. This coincides with large emission increases in Asia suggesting that the recent development in Asia has some influence on the SH.

3.4 Methane evolution and emission drivers over distinct time periods

Fig. 11 compares the latitudinal distribution of surface CH_4 in the model and observations. Generally, the model and the observational approach reveal the same pattern and characteristics both in time and space although some clear differences are evident. From 1985 to the early nineties, there is a homogeneous growth in the observations (Fig. 11b). The model (Fig. 11a) also has growth over the same period but a distinct period (1987-88) with no growth, corresponding to smaller emissions from wetlands and biomass burning (Figure 1). 1987-1988 were El Niño years and there is a tendency of low wetland emissions for those years, e.g. an anti-correlation between wetland emissions and ENSO index (Hodson et al., 2011). It might be that our applied emission inventory for natural CH_4 sources (Bousquet et al., 2011) has too large variability in wetland emissions in the eighties and too strong reductions in wetland emissions in 1987-88. Bousquet et al. (2006) states that bias in OH inferred from methyl chloroform (CH_3CCl_3) observations (Bousquet et al., 2005) could account for some of the variability that they attributed to wetland emissions. Later findings (Montzka et al., 2011) support this. If OH changes are set to zero instead of the large variability in the eighties, suggested by early CH_3CCl_3 studies (Bousquet et al., 2005), the fluctuations in wetland emissions are dampened by 50 %. On the other hand, the model simulation has no year-to-year variation in meteorology before 1997, and the meteorology used corresponds to the year 2001, which has a weak ENSO index. Therefore, during the 1987-1988 El Niño, the meteorology used is less representative than for other years with weaker ENSO. In the two periods of CH_4 growth before and after 1987-88, the CH_4 increase is strong in the model (Fig. 11a) in the Northern Hemisphere and might be overestimated. However, it might be that the model is able to better capture latitudinal gradients, as only a few measurement sites are available to make latitudinal averages for the eighties. In 1992 and 1993 there is a pause in the CH_4 growth in the measurements (Fig. 11b) at all latitudes. This

pause has been explained as a consequence of the Mount Pinatubo volcanic eruption in 1991 (Dlugokencky et al., 1996;Bekki and Law, 1997;Bândă et al., 2013). The eruption results in an initial increase in the CH_4 growth rate (less OH) lasting for half a year. This is due to backscattering by volcanic stratospheric aerosols, which reduces the UV radiation to the troposphere. After that, the growth rate due to Pinatubo becomes negative (more OH plus less natural methane emissions are the dominating effects) reaching a minimum after 2 years (1993), before levelling off towards zero after 5 years. The main cause of the OH increase is reduction in stratospheric ozone allowing more UV radiation to the troposphere. In contrast to the measurements the model shows a stronger decrease in CH_4 after the eruption, and the pause in CH_4 growth is longer. This might be due the fact that the model does not fully include all factors affecting CH_4 related to the Mount Pinatubo eruption. Reduced emissions are implicitly included in the natural CH_4 emission inventories, but changes in meteorology (temperature, water vapor, etc.) and volcanic SO_2 and sulphate aerosols in the stratosphere, are not accounted for in the simulations. In the period 1994-1997 the model struggles to reproduce the latitudinal distribution of growth (Fig. 11). The model seems to have too large growth in the Tropics probably due to a small but significant growth in wetland and biomass burning emissions in the period (Fig. 1).

In the next paragraphs, we study whether the model is able to reproduce CH_4 measurements when we split the time frame into shorter epochs that measured distinct different growth rates. The splits are made within the period 1998-2009 when our simulations have both inter-annual variation in meteorology and complete emission data (no extrapolations made). We have only included observation sites that have measurements available for all months within the given time period, see section 2.3 for details about data selection.

Fig. 12 shows the modelled CH_4 growth in the CTM in the period 1998-2000, compared to the observed changes at various sites. The model seems to slightly underestimate increases at several stations. The largest underestimation occur in eastern Asia. In parts of eastern Asia and some other regions in the Northern Hemisphere there are decline in modelled CH_4 concentrations caused by decreased contribution from several anthropogenic sectors. Increased emissions from gas fields in Russia and the Middle East and in several anthropogenic tracers over India explain why these are the regions in the Northern Hemisphere with largest modelled CH_4 increase.

Earlier studies find that a low CH_4 growth rate in the nineties is mostly caused by lower fugitive fossil fuel emissions from oil and gas industries, mainly due to the collapse of the Soviet Union (Bousquet et al., 2006;Simpson et al., 2012;Dlugokencky et al., 2003;Aydin et al., 2011) . Another important factor is decreased emissions from rice paddies. Lower emissions from agricultural soils last until around year 2000 in the EDGAR v4.2 inventory (Figure 1) and are also evident in Fig. 12c. Kai et al. (2011) exclude fossil fuel emissions as the primary cause of the slowdown of CH_4 growth. According to their isotopic studies, it is more likely long-term reductions in agricultural emissions from rice crops in Asia, or alternatively another microbial source in the Northern Hemisphere that is the major factor. Another isotope study (Levin et al., 2012) disagrees and finds that both fossil and microbial emissions were quite stable.

Wetland and biomass burning sources seem to play the key role for the variations in the model from 1997 to 2000 (Fig. 12a). They were particularly large in 1998 due to the 1997-1998 El Niño (Chen and Prinn, 2006;Simpson et al., 2002;Dlugokencky et al., 2001;Bousquet et al., 2006;Pison et al., 2013;Spahni et al., 2011;Hodson et al., 2011). Simpson et al. (2002) also conclude that the increase in observed surface CH_4 between 1996 and 2000 was driven primarily by a large growth in 1998. Both model and measurements have the strongest growth (Fig. 12) in the Southern Hemisphere, which had large wetland emissions in 1998 (Bousquet et al., 2006;Dlugokencky et al., 2001). In the model, slowly rising anthropogenic emissions in the Southern Hemisphere also seems to contribute (Fig. 12b-f). Natural emissions (Fig. 12a) are also important for the irregular pattern seen at mid-to-high northern latitudes. This is expected due to the 1997-1998 ENSO-event, showing a dip in high northern wetland emissions in 1997 followed by unusual large emissions in 1998 (Bousquet et al., 2006;Dlugokencky et al., 2001). During the ENSO event, the zonal pattern in the model and measurements (Fig. 11) is very similar for the Southern Hemisphere but there are larger differences for the Northern Hemisphere.

During 2000-2006 the CH_4 growth levelled off and there was a period with stagnation in global mean growth rate (Fig. 13). The agreement between the zonal averages from the model and the measurement approach is excellent, both with regards to timing and strength of the growth (Fig. 11 and 13). The 2002-2003 anomaly in the Northern Hemisphere is captured by the model (Fig. 11) and explained by enhanced emissions from biomass burning in Indonesia and boreal Asia (Bergamaschi et al., 2013;Simpson et al., 2006;van der Werf et al., 2010).

The EDGAR v4.2 inventory applied here and in other studies (e.g. Bergamaschi et al., 2013) show that global anthropogenic emissions rise substantially, especially in Asia after year 2000. This increase in the anthropogenic emissions is compensated by a drop in northern tropical wetland emissions associated with years of dry conditions (Bousquet et al., 2006;Bousquet et al., 2011). Monteil et al. (2011) finds that moderate increases in anthropogenic emissions and decreased wetland emissions together with moderate increasing OH can explain the stagnation in CH_4 growth from 2000. Bergamaschi et al. (2013), assuming constant OH, also finds a decrease in wetland emissions but that a large increase in anthropogenic emissions first occurs from 2006 and beyond. Uncertainty in wetland emissions in the period is well illustrated by Pison et al. (2013). Using different methods to estimate global wetland emissions from 2000 to 2006 Pison et al. (2013) finds either a decrease or increase. They find the latter to be most likely, and this question the large increase found in anthropogenic bottom up inventories after 2000. On the other hand, increase in both wetland and anthropogenic emission would not conform to the observed stable global mean CH_4 levels in this period. Spahni et al. (2011) found a small decrease in wetland emissions from 1999-2004 followed by an increase from 2004 to 2008. Our model results from simulations with declining natural emissions and increasing anthropogenic emissions (Fig. 1) reproduce the measurements in most regions (Fig. 13). Eastern Asian stations are exceptions. Gas and solid fuels (coal) (Fig. 13d, e) are causing much of the modelled increases over southern and eastern Asia. Since the observation at the eastern Asian stations close to large anthropogenic sources show smaller changes it is plausible that the emission growth is too strong in the applied EDGAR v4.2 inventory, for this region. However, it is difficult to be conclusive since the few observation sites available are situated in zones with sharp gradients in modelled concentration changes. The EDGAR v4.2 emissions from the region increase gradually between 2000 and 2008, with a larger growth rate after 2002. Findings from Bergamaschi et al. (2013) question this as they suggest a large increase mostly since 2006.

The period 2007 to 2009 is characterized by strong growth in observed global mean growth rate and even stronger growth in the model (Fig. 11 and 14). The model overestimation seems to occur almost everywhere. Due to the long lifetime of CH_4, strong increase in regional emissions has global impact. Increases in anthropogenic sources in Asia (e.g. Fig. 9, Fig. 14b-f), in particular, natural gas in the Middle East and solid fuel (coal) in eastern Asia have large contributions. The influence from emission increases in these regions can be seen at downwind stations over and near northern America and in the Southern Hemisphere

(Seychelles) (see Fig. 6 and 7). For the Southern Hemisphere a small steady increase in several regional anthropogenic emissions also contributes. For the Arctic stations the responsible sectors for the recent increase and their geographical origin varies but high wetland emissions in 2007-2008, gas in Russia, and coal and other anthropogenic emissions in Asia seem to play a central roles (Fig. 7, 8 and 14). For North America anthropogenic emissions increase in central and eastern U.S. and decrease in the eastern parts (Fig. 14). A similar west-east gradient is seen over the continent for natural sources but this is likely temporary due to special conditions in 2007-2008. These factors, together with the distant contributions from rising emissions in eastern Asia explain the modelled CH_4 trends. In central Europe there is a decline in modelled CH_4 due to a combination of declining emissions from enteric fermentation, solid fuels (coal), and several other anthropogenic sectors (Fig. 14 b,d,f), and fluctuations in natural emissions (Fig. 14a). A decrease over a small region of South America is mainly explained by variations in natural emissions (Fig. 14a).

Other studies (Kirschke et al., 2013;Rigby et al., 2008;Bergamaschi et al., 2013;Bousquet et al., 2011;Dlugokencky et al., 2009;Crevoisier et al., 2013;Bruhwiler et al., 2014) attribute the resumed strong growth of observed (Dlugokencky et al., 2009;Rigby et al., 2008;Frankenberg et al., 2011;Sussmann et al., 2012;Crevoisier et al., 2013) global CH_4 levels after 2006 to increases in both natural and anthropogenic emissions. However, the share of natural versus anthropogenic contribution varies in the different studies. The studies agree that abnormally high temperatures at high northern latitudes in 2007 and increased tropical rainfall in 2007 and 2008 resulted in large wetland emissions these years. There is also a likely contribution from forest fires in the autumn of 2006 due to drought in Indonesia (Bergamaschi et al., 2013;Worden et al., 2013). Top down (Bergamaschi et al., 2013;Bousquet et al., 2006;Bousquet et al., 2011;Kirschke et al., 2013;Bruhwiler et al., 2014) and bottom up studies (EC-JRC/PBL, 2011;Schwietzke et al., 2014;Höglund-Isaksson, 2012;EPA, 2012) suggest steady moderate to substantial increases in anthropogenic emissions in the period 2007-2009. Much of this is due to intensification of oil and shale gas extraction in the United States and coal exploitation in China.

Using the EDGAR v4.0 inventory as input to a CTM and observations of CH_4 and its isotopic composition Monteil et al. (2011) concluded that a reduction of biomass burning and/or of the growth rate of fossil fuel emissions is needed to explain the observed growth after 2005. The differences between the EDGAR v4.0 and EDGAR v4.2 used in this study are moderate. Other bottom up inventories (EPA, 2012;Höglund-Isaksson, 2012;Schwietzke et al., 2014)

report lower increases in anthropogenic emissions, see also comparison with ECLIPSE emission in the supplement. Using the mean of the EPA and EDGAR v4.2 inventory for anthropogenic emissions Kirschke et al. (2013) finds that either is the increase in fossil fuel emissions overestimated by inventories, or the sensitivity of wetland emissions to temperature and precipitation is too large in wetland emission models. Schwietzke et al. (2014) and the top-down studies by Bergamaschi et al. (2013) and Bruhwiler et al. (2014) conclude that the EDGAR v4.2 emission inventory overestimates the recent emission growth in Asia. This is especially the case for coal mining in China. From our results above it is plausible that too high growth of fossil fuel emissions, in particular in Asia, is the reason why the recent CH_4 growth is higher in our model than for the observations. However, in 2007 and 2008 much of the increase in the model in the Northern Hemisphere is driven by high natural wetland emissions. Our natural emissions are from Bousquet et al. (2011) who attributes much of the 2007-2008 increase in total emissions to wetlands. According to Bergamaschi et al. (2013) a substantial fraction of the total increase is attributed to anthropogenic emissions. There is therefore a possibility that we combine two emission inventories (anthropogenic from EDGAR v4.2 and natural from Bousquet et al.) that both have too large growth in the period 2006-2008.

Extrapolating anthropogenic emissions that likely have too strong growth probably explain why the model also overestimates the CH_4 growth from 2009 to 2012. Mismatch between the spatial distributions of the model and measurements (Fig. 11) on regional scales from 2009 to 2012 are expected due to the extrapolation of anthropogenic emissions and use of constant 2009 natural and biomass burning emissions. Of these, especially wetland emissions have large spatial and temporal variation from year to year.

3.5 Changes in methane lifetime

The modelled evolution of CH_4 is not only decided by changes in sources but also changes in the atmospheric CH_4 loss and soil uptake. The CH_4 lifetime is an indicator of the CH_4 loss. The lifetime is dependent on the efficiency of soil uptake (Curry, 2009), and concentrations of atmospheric chemical components reacting with CH_4, including the kinetic rates of the corresponding reactions. It also depends on how efficiently the emitted CH_4 is transported between regions with differences in loss rate. Our prescribed fields for soil uptake (Bousquet et al., 2011) are responsible for about 5 % of the loss and the difference between the year with smallest and largest soil uptake is only 2 %. The main reactant removing CH_4 chemically in the atmosphere is OH, but there is also a small loss due to reactions with excited atomic

oxygen (O^1D) and chlorine (Lelieveld et al., 1998;Crutzen, 1991). Due to the limited influence of soil uptake, chlorine, and O^1D we will hereafter focus on the role of changes in OH and the kinetic loss rate for this reaction. A number of components (CO, NOx, NMVOCs, CH_4, SO_2, aerosols, meteorological factors, solar radiation) control the atmospheric OH level and the kinetic loss rate (Dalsøren and Isaksen, 2006;Lelieveld et al., 2004;Holmes et al., 2013;Levy, 1971). Due to the extremely high reactivity of OH, measurements on large scale are impossible (Heard and Pilling, 2003). Forward models have been employed to calculate the OH evolution over time on global scale. Another alternative is inverse models in combination with observations of ^{14}CO , CH_3CCl_3 or other long-lived species reacting with OH. This section discusses the modelled evolution of CH_4 lifetime in this study and compares it to findings from other relevant studies on CH_4 lifetime and OH change. In the section thereafter we try to identify the key drivers behind the modelled changes in CH_4 lifetime.

The overall picture from the main simulation (blue lines Fig. 15) is that there is a clear decrease in the CH_4 lifetime over the last four decades, more than 8% from 1970 to 2012 and a similar increase in OH concentration. Of particular importance is large increases in OH over Southeast Asia, mainly due to strong growth in NO_x emissions. From 2000-2010 the modelled tropospheric OH column increase by 10-20 % over China and India (not shown). In Fig. 15, the reaction rate with methane is used as averaging kernel to examine the OH change relevant for changes in methane lifetime. There is a very strong anti-correlation between the evolution of OH and methane lifetime suggesting causality. This is especially the case for the period 1970-1997 run without inter-annual variation in meteorology resulting in a static CH_4+OH reaction rate (k) for these years. The lifetimes in the fixed CH_4 run (red line) and the main CH_4 run (blue line) are highly correlated. This is another way of illustrating that OH (k x OH), and not the CH_4 burden itself, is driving the long-term evolution and year-to-year variations of CH_4 lifetime. However, some influence from CH_4 fluctuations is evident in a few years (mainly in the eighties) with large variations in CH_4 emissions (Fig. 1). CH_4 itself is important for its own lifetime length (blue line well above red line), due to the decrease in the OH concentration produced by the reaction with the CH_4.

Other forward models also suggest similar decrease in CH_4 lifetime due to increase in global OH concentrations the recent decades (Karlsdóttir and Isaksen, 2000;Dentener et al., 2003;Wang et al., 2004;Dalsøren and Isaksen, 2006;Fiore et al., 2006;John et al., 2012;Holmes et al., 2013;Naik et al., 2013). However, some of these studies focus on the effect of certain factors (emissions or meteorology) and do not cover changes in all central

physical and chemical parameters affecting CH_4 lifetime. Using observations of CH_4 and its isotopic composition, Monteil et al. (2011) find that moderate (<5 % per decade) increases in global OH over the period 1980-2006 are needed to explain the observed slowdown in the growth rate of atmospheric CH_4 at the end of that period. In contrast large increases in OH in the 1980s and a large negative trend for the 1990s were inferred from CH_3CCl_3 observations (Prinn et al., 2005;Prinn et al., 2001;Krol and Lelieveld, 2003;Bousquet et al., 2005;Montzka et al., 2000). These studies also found large inter-annual variability of OH. However, the studies were debated (Krol and Lelieveld, 2003;Lelieveld et al., 2006;Bousquet et al., 2005;Wang et al., 2008) and it was shown that largely reduced variations and trends are possible within the uncertainties bonds of the CH_3CCl_3 emission inventory. In a more recent analysis of CH_3CCl_3 measurements for the period 1998-2007 Montzka et al. (2011) find small inter-annual OH variability and trends and attribute previously estimated large year-to-year OH variations before 1998 to uncertainties in CH_3CCl_3 emissions and representation issues given sparse observation network. Kai et al. (2011) finds that relatively stable dD-CH_4 suggested small changes in the OH sink between 1998 and 2005. Rigby et al. (2008) finds declining OH from 2004 to 2007. Bousquet et al. (2011) also finds a decline in 2007 and 2008, compared to 2006. However the decline is much less than that found by Rigby et al. Holmes et al. (2013) concludes that better understanding of systematic differences between different CH_3CCl_3 observation networks is required before using them as constraints on inter-annual variability of CH_4 lifetime and OH. Using ^{14}CO Manning et al. (2005) finds no significant long term trend in OH in the Southern Hemisphere but short term large variations persisting for a few months. Like CH_3CCl_3 there are uncertainties related to inferring OH from ^{14}CO (Krol et al., 2008). Ghosh et al. (2015) does not consider trends in OH but anyway they find a decrease in CH_4 lifetime over the last century and attribute it to temperature increase (larger reaction rate) and the increase of stratospheric chlorine (larger loss through reaction with Cl).

It is evident from the above discussion that there are uncertainties related to all methods (models, CH_3CCl_3, and ^{14}CO) and missing consensus on OH trends. To increase understanding and facilitate discussion it is important not to stop by a derived number for change in OH or methane lifetime, but investigate the major drivers for the changes. The next section address drivers in this model study.

3.6 Major drivers for changes in the methane lifetime

Fig. 16 shows the evolution of main factors known to determine atmospheric CH_4 lifetime. The factors chosen are based on the study by Dalsøren and Isaksen (2006) and Holmes et al. (2013).

Using the NOx/CO emission ratio and linear regression analysis (Dalsøren and Isaksen, 2006) found a simple equation describing the evolution of OH resulting from emission changes in the period 1990-2001. In general, CO emission increases lead to an overall reduction in current global averaged OH levels. An increase in NO_x emissions increases global OH as long as it takes place outside highly polluted regions. In this study the general picture is that the NOx/CO emission ratio increases over the 1970-2012 period (Fig. 16). Despite the general increase, periods of declining ratio can be seen both after the oil crisis in 1973 and the energy crisis in 1979. This occurs since NOx emissions are more affected than CO emissions. After 1997 when we include year to year variation in emissions from vegetation fires the NOx/CO emission ratio is more variable. Large drops in ratio can be seen in years with high incidences of fires resulting in large CO emissions. This is typical for ENSO episodes (1997-1998) and warm years (2010). Agreement with observed CO trends (see comparison in Supplement section S5) indicates that the modelled changes of CO and OH, and applied CO emissions are internally consistent.

Holmes et al. (2013) found formulas for predicting CH_4 lifetime due to changes in meteorology using some of the factors shown in Fig. 16. It is only from 1997 that our simulations include inter-annual variation in meteorology. We find that variations in global averaged specific humidity and temperature are highly correlated with each other and a 6 month delayed ENSO index. This is reasonable as this is a typical response time for physical and chemical signals to propagate from one hemisphere to the other. High temperature and specific humidity, meaning high water vapor content, is for instance found in the ENSO year 1998 and warm year 2010 (Fig. 16). Variations in these parameters are important for the CH_4 lifetime since the reaction rate (k) between OH and CH_4 is highly temperature dependent and water vapor is a precursor of OH (Levy, 1971). The production of OH is also dependent on UV radiation and thereby the atmospheric ozone column absorbing such radiation (Rohrer and Berresheim, 2006). The highest UV radiation is found at low latitudes and the ozone burden between 40°S and 40° N is regarded as a useful indicator (Holmes et al., 2013). The emissions of NO_x from lightning are dependent on a number of meteorological factors and thereby quite variable from year to year (Fig. 16).

In this section we investigate whether simplified expressions for the evolution of CH_4 lifetime can be found based on the parameters in Fig. 16. Such equations could be very useful for fast prediction of future development of CH_4 lifetime and CH_4 burden. Since we study different time periods than Dalsøren and Isaksen (2006) and Holmes et al. (2013) and both emissions and meteorology are perturbed in our simulations, it is not obvious that simplified equations would be statistically valid.

Fig. 17 shows the results of multiple linear regression analysis performed to describe the CH_4 lifetime over the period 1970 to 1996. For this period fixed year to year meteorology was used in the main model simulation. This means that parameters like lightning NO_x, temperature and specific humidity (Fig. 16) can be kept out of the regression analysis. The equation best reproducing (R^2=0.99) the lifetime evolution from the main run (Fig. 17) and having statistical significant linear relations between its parameters and CH_4 lifetime is:

$$CH_4 \text{ lifetime (yr)} = 11.9 - 21.4 \times (NO_x/CO)_{emissions}.$$

This confirms the analysis from previous sections suggesting that CH_4 itself has small influence on the variation in CH_4 lifetime during this period. The same seems to be the case for variations in ozone column. A similar simple equation was found by Dalsøren and Isaksen (2006). This suggests that near future variation of CH_4 lifetime due to changes in emissions can be predicted solely by looking at the ratio of NOx to CO emissions. However, it should be noted that the region of emission change is important (Berntsen et al., 2006). This is especially the case for NO_x emissions due to the short atmospheric NO_x lifetime. For instance, changes in NO_x emissions at low latitudes with moderate pollution levels (OH response is non-linear) would have profound impacts on CH_4 lifetime due to the temperature dependency of the reaction between CH_4 and OH.

The blue line in Fig. 18 shows the lifetime over the period 1997-2012 as predicted by the main model run. The red line shows the best fit from a simple parametric model. Because the main CTM run for this period include year to year variation in meteorology, the simple regression model need more parameters to reproduce the evolution. Still a simplified equation (R^2=0.99) is statistically valid predicting the CH_4 lifetime by a linear combination of the parameters specific humidity (q), NO_x/CO emission ratio $(NO_x/CO)_e$, lightning NO_x emissions $(LNO_x)_e$, and O_3 column:

$$CH_4 \text{ lifetime (yr)} = 0.07 \times O_{3column} - 4.80 \times (NO_x/CO)_e - 0.04 \times q - 1.21 \times (LNOx)_e.$$

It should be noted that specific humidity and temperature have almost identical year to year variation and it is therefore not given which of these parameters that should be used.

4 Summary and conclusions

Uncertainties in physical and chemical processes in models, input data on emissions and meteorology, and limited spatial and temporal coverage of measurement data, have made it hard for both bottom up and top down studies to settle the global CH_4 budget, untangle the causes for recent trends, and predict future evolution (Ciais et al., 2013;Kirschke et al., 2013;Nisbet et al., 2014). As the quality and detail level of models, input data, and measurements progress, the chances of understanding more pieces in the big puzzle increase. This study is an effort in such a perspective.

In our bottom up approach, a global Chemical Transport Model (CTM) was used to study the evolution of atmospheric CH_4 over the period 1970-2012. The study includes a thorough comparison with CH_4 measurements from surface stations covering all regions of the globe. The seasonal variations are reproduced at most stations. The model also reproduces much the observed evolution of CH_4 on both inter-annual and decadal time scales. Variations in wetland emissions are the major drivers for year-to-year variation of CH_4. Regarding trends, the causes are much debated as discussed in the previous sections. Consensus is not reached on the relative contribution from individual emission sectors, neither on the share of natural versus anthropogenic sources. The fact that our simulations capture much of the observed regional changes indicates that our transport and chemistry schemes perform well and that applied emission inventories are reasonable with regard to temporal, spatial, sectoral, and natural versus anthropogenic distribution of emissions. However, there are some larger discrepancies in model performance questioning the accuracy of the CH_4 emission data in certain regions and periods. Potential flaws in emission data are pinpointed for recent years when our model simulations are more complete with regard to input data (e.g. emissions, variable meteorology, etc.) and there are more measurements available for comparison. After a period of stable CH_4 levels from 2000-2006, observations show increasing levels from 2006 in both hemispheres. From 2006, the model overestimates the growth in all regions, in particular in Asia. Large emission growth in Asia influences the CH_4 trends in most world regions. Our findings support other studies suggesting that the recent growth in Asian anthropogenic emissions is too high in the EDGAR v4.2 inventory. Based on our model

results and the comparison between ECLIPSE and EDGAR v4.2 emissions in the supplement (S2) we also question the Asian emission trends in the nineties and beginning of the 2000s in the EDGAR v4.2 inventory, although the limited number of measurement sites in Asia makes it difficult to validate this.

The modelled evolution of CH_4 is also dependent on changes in the atmospheric CH_4 loss. The CH_4 lifetime is an indicator of the CH_4 loss. In our simulations, the CH_4 lifetime decreases by more than 8 % from 1970 to 2012. The reason for the large change is increased atmospheric oxidation capacity. Such changes are in theory driven by complex interactions between a number of chemical components and meteorological factors. However, our analysis reveals that key factors for the development are changes in specific humidity, NO_x/CO emission ratio, lightning NO_x emissions, and total ozone column. It is statistically valid to predict the CH_4 lifetime by a combination of these parameters in a simple equation. The calculated change in CH_4 lifetime is within the range reported by most other bottom up model studies. However, findings from these studies do not fully agree with top down approaches using observations of CH_3CCl_3 or ^{14}CO.

Without the calculated increase in oxidation capacity, the CH_4 growth over the last decades would have been much higher. Increasing CH_4 loss also likely contributed to the stagnation of CH_4 growth in the period 2001-2006. Interestingly, over the last few years, the loss deviates from its steady increase over the previous decades. Much of this deviation seems to be caused by variation in meteorology. Our simulations reveal that accounting for variation in meteorology has a strong effect on the atmospheric CH_4 loss. This in turn affects both inter-annual and long term changes in CH_4 burden. A stabilization of the CH_4 loss, mainly due to meteorological variability, likely contributed to a continuing increase (2009-2012) in CH_4 burden after high emission years in 2007 and 2008. Due to the long response time of CH_4 this could also contribute to future CH_4 growth. However, there are extra uncertainties in the model results after 2009 due to lack of comprehensive emission inventories. A new inventory or update of existing ones with sector-vice separation of emission for recent years (2009-2015) would be a very valuable piece for model studies trying to close the gaps in the CH_4 puzzle. It will also provide important fundament for more accurate predictions of future CH_4 levels and various mitigation strategies.

Acknowledgements

This work was funded by the Norwegian Research Council project GAME (Causes and effects of Global and Arctic changes in the Methane budget), grant no. 207587, under the program NORKLIMA, and the EU project ACCESS (Arctic Climate Change Economy and Society). ACCESS received funding from the European Union under grant agreement n° 265863 within the Ocean of tomorrow call of the European Commission seventh framework programme. We are grateful to Phillipe Bousquet for providing and sharing datasets on methane emissions. The work and conclusions of the paper could not been achieved without globally distributed observational data and we acknowledge all data providers, and the great efforts of AGAGE, NOAA ESRL, and The World Data Centre for Greenhouse Gases (WDCGG) under the GAW programme for making data public and available. Specific thanks go to Nina Paramonova, Hsiang J.Wang, Simon O'Doherty,Yasunori Tohjima, Edward J Dlugokencky, who are the PIs of the observation data shown in Fig. 6-10 and 12-14. We also thank Edward J Dlugokencky for sharing the observational based data set for Fig. 11, and WDCGG and Paul Novelli for sharing CO datasets used in Fig. S5 of the supplement.

5 References

Aydin, M., Verhulst, K. R., Saltzman, E. S., Battle, M. O., Montzka, S. A., Blake, D. R., Tang, Q., and Prather, M. J.: Recent decreases in fossil-fuel emissions of ethane and methane derived from firn air, *Nature*, 476, 198-201, http://www.nature.com/nature/journal/v476/n7359/abs/nature10352.html#supplementary-information, 2011.

Bândă, N., Krol, M., van Weele, M., van Noije, T., and Röckmann, T.: Analysis of global methane changes after the 1991 Pinatubo volcanic eruption, *Atmos. Chem. Phys.*, 13, 2267-2281, 10.5194/acp-13-2267-2013, 2013.

Bekki, S., and Law, K. S.: Sensitivity of the atmospheric CH4 growth rate to global temperature changes observed from 1980 to 1992, *Tellus B*, 49, 409-416, 10.1034/j.1600-0889.49.issue4.6.x, 1997.

Bergamaschi, P., Houweling, S., Segers, A., Krol, M., Frankenberg, C., Scheepmaker, R. A., Dlugokencky, E., Wofsy, S. C., Kort, E. A., Sweeney, C., Schuck, T., Brenninkmeijer, C., Chen, H., Beck, V., and Gerbig, C.: Atmospheric CH4 in the first decade of the 21st century: Inverse modeling analysis using SCIAMACHY satellite retrievals and NOAA surface measurements, *Journal of Geophysical Research: Atmospheres*, 118, 7350-7369, 10.1002/jgrd.50480, 2013.

Berglen, T., Berntsen, T., Isaksen, I., and Sundet, J.: A global model of the coupled sulfur/oxidant chemistry in the troposphere: The sulfur cycle, *J. Geophys. Res.: Atmos.*, 109, 27 pp, ARTN D19310

DOI 10.1029/2003JD003948, 2004.

Berntsen, T., Fuglestvedt, J., Myhre, G., Stordal, F., and Berglen, T.: Abatement of Greenhouse Gases: Does Location Matter?, *Clim. Change*, 74, 377-411, 10.1007/s10584-006-0433-4, 2006.

Bhattacharya, S. K., Borole, D. V., Francey, R. J., Allison, C. E., Steele, L. P., Krummel, P., Langenfelds, R., Masarie, K. A., Tiwari, Y. K., and Patra, P. K.: Trace gases and CO2 isotope records from Cabo de Rama, India,, *Current Science*, 97, 1336–1344, 2009.

Bousquet, P., Hauglustaine, D. A., Peylin, P., Carouge, C., and Ciais, P.: Two decades of OH variability as inferred by an inversion of atmospheric transport and chemistry of methyl chloroform, *Atmos. Chem. Phys.*, 5, 2635-2656, 10.5194/acp-5-2635-2005, 2005.

Bousquet, P., Ciais, P., Miller, J. B., Dlugokencky, E. J., Hauglustaine, D. A., Prigent, C., Van der Werf, G. R., Peylin, P., Brunke, E. G., Carouge, C., Langenfelds, R. L., Lathiere, J., Papa, F., Ramonet, M., Schmidt, M., Steele, L. P., Tyler, S. C., and White, J.: Contribution of anthropogenic and natural sources to atmospheric methane variability, *Nature*, 443, 439-443, http://www.nature.com/nature/journal/v443/n7110/suppinfo/nature05132_S1.html, 2006.

Bousquet, P., Ringeval, B., Pison, I., Dlugokencky, E. J., Brunke, E. G., Carouge, C., Chevallier, F., Fortems-Cheiney, A., Frankenberg, C., Hauglustaine, D. A., Krummel, P. B., Langenfelds, R. L., Ramonet, M., Schmidt, M., Steele, L. P., Szopa, S., Yver, C., Viovy, N., and Ciais, P.: Source attribution of the changes in atmospheric methane for 2006–2008, *Atmos. Chem. Phys.*, 11, 3689-3700, 10.5194/acp-11-3689-2011, 2011.

Bridgham, S. D., Cadillo-Quiroz, H., Keller, J. K., and Zhuang, Q.: Methane emissions from wetlands: biogeochemical, microbial, and modeling perspectives from local to global scales, *Global Change Biology*, 19, 1325-1346, 10.1111/gcb.12131, 2013.

Bruhwiler, L., Dlugokencky, E., Masarie, K., Ishizawa, M., Andrews, A., Miller, J., Sweeney, C., Tans, P., and Worthy, D.: CarbonTracker-CH4: an assimilation system for estimating emissions of atmospheric methane, *Atmos. Chem. Phys.*, 14, 8269-8293, 10.5194/acp-14-8269-2014, 2014.

Chen, Y.-H., and Prinn, R. G.: Estimation of atmospheric methane emissions between 1996 and 2001 using a three-dimensional global chemical transport model, *Journal of Geophysical Research: Atmospheres*, 111, D10307, 10.1029/2005JD006058, 2006.

Ciais, P., Sabine, C., Bala, G., Bopp, L., Brovkin, V., Canadell, J., Chhabra, A., DeFries, R., Galloway, J., Heimann, M., Jones, C., Le Quéré, C., Myneni, R. B., Piao, S., and Thornton, P.: Carbon and Other Biogeochemical Cycles, in: Climate Change 2013: The Physical Science Basis. Contribution of Working Group I to the Fifth Assessment Report of the Intergovernmental Panel on Climate Change, edited by: Stocker, T. F., Qin, D., Plattner, G.-K., Tignor, M., Allen, S. K., Boschung, J., Nauels, A., Xia, Y., Bex, V., and Midgley, P. M., Cambridge University Press, Cambridge, United Kingdom and New York, NY, USA, 465–570, 2013.

Crevoisier, C., Nobileau, D., Armante, R., Crépeau, L., Machida, T., Sawa, Y., Matsueda, H., Schuck, T., Thonat, T., Pernin, J., Scott, N. A., and Chédin, A.: The 2007–2011 evolution of tropical methane in the mid-troposphere as seen from space by MetOp-A/IASI, *Atmos. Chem. Phys.*, 13, 4279-4289, 10.5194/acp-13-4279-2013, 2013.

Crutzen, P. J.: Methane's sinks and sources, *Nature*, 350, 380-381, 1991.

Curry, C. L.: The consumption of atmospheric methane by soil in a simulated future climate, *Biogeosciences*, 6, 2355-2367, 10.5194/bg-6-2355-2009, 2009.

Dalsoren, S., Eide, M., Myhre, G., Endresen, O., Isaksen, I., and Fuglestvedt, J.: Impacts of the Large Increase in International Ship Traffic 2000-2007 on Tropospheric Ozone and Methane, *Environ. Sci. Technol.*, 2482-2489, DOI 10.1021/es902628e, 2010.

Dalsøren, S. B., and Isaksen, I. S. A.: CTM study of changes in tropospheric hydroxyl distribution 1990–2001 and its impact on methane, *Geophysical Research Letters*, 33, L23811, 10.1029/2006GL027295, 2006.

Dalsøren, S. B., Isaksen, I. S. A., Li, L., and Richter, A.: Effect of emission changes in Southeast Asia on global hydroxyl and methane lifetime, *Tellus B*, 61, 10.3402/tellusb.v61i4.16857, 2011.

Dentener, F., van Weele, M., Krol, M., Houweling, S., and van Velthoven, P.: Trends and inter-annual variability of methane emissions derived from 1979-1993 global CTM simulations, *Atmos. Chem. Phys.*, 3, 73-88, 10.5194/acp-3-73-2003, 2003.

Dlugokencky, E. J., Dutton, E. G., Novelli, P. C., Tans, P. P., Masarie, K. A., Lantz, K. O., and Madronich, S.: Changes in CH4 and CO growth rates after the eruption of Mt. Pinatubo and their link with changes in tropical tropospheric UV flux, *Geophysical Research Letters*, 23, 2761-2764, 10.1029/96GL02638, 1996.

Dlugokencky, E. J., Walter, B. P., Masarie, K. A., Lang, P. M., and Kasischke, E. S.: Measurements of an anomalous global methane increase during 1998, *Geophysical Research Letters*, 28, 499-502, 10.1029/2000GL012119, 2001.

Dlugokencky, E. J., Houweling, S., Bruhwiler, L., Masarie, K. A., Lang, P. M., Miller, J. B., and Tans, P. P.: Atmospheric methane levels off: Temporary pause or a new steady-state?, *Geophysical Research Letters*, 30, 1992, 10.1029/2003GL018126, 2003.

Dlugokencky, E. J., Bruhwiler, L., White, J. W. C., Emmons, L. K., Novelli, P. C., Montzka, S. A., Masarie, K. A., Lang, P. M., Crotwell, A. M., Miller, J. B., and Gatti, L. V.: Observational constraints on recent increases in the atmospheric CH4 burden, *Geophysical Research Letters*, 36, L18803, 10.1029/2009GL039780, 2009.

EC-JRC/PBL. Emission Database for Global Atmospheric Research (EDGAR), release version 4.2.: http://edgar.jrc.ec.europa.eu, 2011.

EPA: Global Anthropogenic Non-CO2 Greenhouse Gas Emissions: 1990–2030, U.S. Environmental Protection Agency Washington, DC, 2012.

Fiore, A. M., Horowitz, L. W., Dlugokencky, E. J., and West, J. J.: Impact of meteorology and emissions on methane trends, 1990–2004, *Geophysical Research Letters*, 33, n/a-n/a, 10.1029/2006GL026199, 2006.

Fiore, A. M., West, J. J., Horowitz, L. W., Naik, V., and Schwarzkopf, M. D.: Characterizing the tropospheric ozone response to methane emission controls and the benefits to climate and air quality, *Journal of Geophysical Research: Atmospheres*, 113, D08307, 10.1029/2007JD009162, 2008.

Fiore, A. M., Naik, V., Spracklen, D. V., Steiner, A., Unger, N., Prather, M., Bergmann, D., Cameron-Smith, P. J., Cionni, I., Collins, W. J., Dalsoren, S., Eyring, V., Folberth, G. A., Ginoux, P., Horowitz, L. W., Josse, B., Lamarque, J.-F., MacKenzie, I. A., Nagashima, T., O'Connor, F. M., Righi, M., Rumbold, S. T., Shindell, D. T., Skeie, R. B., Sudo, K., Szopa, S., Takemura, T., and Zeng, G.: Global air quality and climate, *Chem. Soc. Rev.*, 41, 6663-6683, 10.1039/C2CS35095E, 2012.

Fisher, R. E., Sriskantharajah, S., Lowry, D., Lanoisellé, M., Fowler, C. M. R., James, R. H., Hermansen, O., Lund Myhre, C., Stohl, A., Greinert, J., Nisbet-Jones, P. B. R., Mienert, J., and Nisbet, E. G.: Arctic methane sources: Isotopic evidence for atmospheric inputs, *Geophysical Research Letters*, 38, L21803, 10.1029/2011GL049319, 2011.

Frankenberg, C., Aben, I., Bergamaschi, P., Dlugokencky, E. J., van Hees, R., Houweling, S., van der Meer, P., Snel, R., and Tol, P.: Global column-averaged methane mixing ratios from 2003 to 2009 as derived from SCIAMACHY: Trends and variability, *Journal of Geophysical Research: Atmospheres*, 116, D04302, 10.1029/2010JD014849, 2011.

Ghosh, A., Patra, P. K., Ishijima, K., Umezawa, T., Ito, A., Etheridge, D. M., Sugawara, S., Kawamura, K., Miller, J. B., Dlugokencky, E. J., Krummel, P. B., Fraser, P. J., Steele, L. P., Langenfelds, R. L., Trudinger, C. M., White, J. W. C., Vaughn, B., Saeki, T., Aoki, S., and Nakazawa, T.: Variations in global methane sources and sinks during 1910–2010, *Atmos. Chem. Phys.*, 15, 2595-2612, 10.5194/acp-15-2595-2015, 2015.

Guenther, A., Karl, T., Harley, P., Wiedinmyer, C., Palmer, P. I., and Geron, C.: Estimates of global terrestrial isoprene emissions using MEGAN (Model of Emissions of Gases and Aerosols from Nature), *Atmos. Chem. Phys.*, 6, 3181-3210, 10.5194/acp-6-3181-2006, 2006.

Heard, D. E., and Pilling, M. J.: Measurement of OH and HO2 in the Troposphere, *Chem. Rev.*, 103, 5163-5198, 10.1021/cr020522s, 2003.

Hodson, E. L., Poulter, B., Zimmermann, N. E., Prigent, C., and Kaplan, J. O.: The El Niño–Southern Oscillation and wetland methane interannual variability, *Geophysical Research Letters*, 38, L08810, 10.1029/2011GL046861, 2011.

Holmes, C. D., Prather, M. J., Søvde, O. A., and Myhre, G.: Future methane, hydroxyl, and their uncertainties: key climate and emission parameters for future predictions, *Atmos. Chem. Phys.*, 13, 285-302, 10.5194/acp-13-285-2013, 2013.

Houweling, S., Krol, M., Bergamaschi, P., Frankenberg, C., Dlugokencky, E. J., Morino, I., Notholt, J., Sherlock, V., Wunch, D., Beck, V., Gerbig, C., Chen, H., Kort, E. A., Röckmann, T., and Aben, I.: A multi-year methane inversion using SCIAMACHY, accounting for systematic errors using TCCON measurements, *Atmos. Chem. Phys.*, 14, 3991-4012, 10.5194/acp-14-3991-2014, 2014.

Höglund-Isaksson, L.: Global anthropogenic methane emissions 2005–2030: technical mitigation potentials and costs, *Atmos. Chem. Phys.*, 12, 9079-9096, 10.5194/acp-12-9079-2012, 2012.

Isaksen, I., Berntsen, T., Dalsøren, S., Eleftheratos, K., Orsolini, Y., Rognerud, B., Stordal, F., Søvde, O., Zerefos, C., and Holmes, C.: Atmospheric Ozone and Methane in a Changing Climate, *Atmosphere*, 5, 518-535, 2014.

Isaksen, I. S. A., Gauss, M., Myhre, G., Walter Anthony, K. M., and Ruppel, C.: Strong atmospheric chemistry feedback to climate warming from Arctic methane emissions, *Global Biogeochem. Cycles*, 25, GB2002, 10.1029/2010GB003845, 2011.

John, J. G., Fiore, A. M., Naik, V., Horowitz, L. W., and Dunne, J. P.: Climate versus emission drivers of methane lifetime against loss by tropospheric OH from 1860–2100, *Atmos. Chem. Phys.*, 12, 12021-12036, 10.5194/acp-12-12021-2012, 2012.

Johnson, C. E., Stevenson, D. S., Collins, W. J., and Derwent, R. G.: Interannual variability in methane growth rate simulated with a coupled Ocean-Atmosphere-Chemistry model, *Geophysical Research Letters*, 29, 9-1-9-4, 10.1029/2002GL015269, 2002.

Kai, F. M., Tyler, S. C., Randerson, J. T., and Blake, D. R.: Reduced methane growth rate explained by decreased Northern Hemisphere microbial sources, *Nature*, 476, 194-197, http://www.nature.com/nature/journal/v476/n7359/abs/nature10259.html#supplementary-information, 2011.

Karlsdóttir, S., and Isaksen, I. S. A.: Changing methane lifetime: Possible cause for reduced growth, *Geophysical Research Letters*, 27, 93-96, 10.1029/1999GL010860, 2000.

Kirschke, S., Bousquet, P., Ciais, P., Saunois, M., Canadell, J. G., Dlugokencky, E. J., Bergamaschi, P., Bergmann, D., Blake, D. R., Bruhwiler, L., Cameron-Smith, P., Castaldi, S., Chevallier, F., Feng, L., Fraser, A., Heimann, M., Hodson, E. L., Houweling, S., Josse, B., Fraser, P. J., Krummel, P. B., Lamarque, J.-F., Langenfelds, R. L., Le Quere, C., Naik, V., O'Doherty, S., Palmer, P. I., Pison, I., Plummer, D., Poulter, B., Prinn, R. G., Rigby, M., Ringeval, B., Santini, M., Schmidt, M., Shindell, D. T., Simpson, I. J., Spahni, R., Steele, L. P., Strode, S. A., Sudo, K., Szopa, S., van der Werf, G. R., Voulgarakis, A., van Weele, M., Weiss, R. F., Williams, J. E., and Zeng, G.: Three decades of global methane sources and sinks, *Nature Geosci*, 6, 813-823, 10.1038/ngeo1955

http://www.nature.com/ngeo/journal/v6/n10/abs/ngeo1955.html#supplementary-information, 2013.

Krol, M., and Lelieveld, J.: Can the variability in tropospheric OH be deduced from measurements of 1,1,1-trichloroethane (methyl chloroform)?, *Journal of Geophysical Research: Atmospheres*, 108, n/a-n/a, 10.1029/2002JD002423, 2003.

Krol, M. C., Meirink, J. F., Bergamaschi, P., Mak, J. E., Lowe, D., Jöckel, P., Houweling, S., and Röckmann, T.: What can 14CO measurements tell us about OH?, *Atmos. Chem. Phys.*, 8, 5033-5044, 10.5194/acp-8-5033-2008, 2008.

Lelieveld, J., Dentener, F. J., Peters, W., and Krol, M. C.: On the role of hydroxyl radicals in the self-cleansing capacity of the troposphere, *Atmos. Chem. Phys.*, 4, 2337-2344, 10.5194/acp-4-2337-2004, 2004.

Lelieveld, J., Brenninkmeijer, C. A. M., Joeckel, P., Isaksen, I. S. A., Krol, M. C., Mak, J. E., Dlugokencky, E., Montzka, S. A., Novelli, P. C., Peters, W., and Tans, P. P.: New Directions: Watching over tropospheric hydroxyl (OH), *Atmos. Environ.*, 40, 5741-5743, http://dx.doi.org/10.1016/j.atmosenv.2006.04.008, 2006.

Lelieveld, J. O. S., Crutzen, P. J., and Dentener, F. J.: Changing concentration, lifetime and climate forcing of atmospheric methane, *Tellus B*, 50, 128-150, 10.1034/j.1600-0889.1998.t01-1-00002.x, 1998.

Levin, I., Veidt, C., Vaughn, B. H., Brailsford, G., Bromley, T., Heinz, R., Lowe, D., Miller, J. B., Posz, C., and White, J. W. C.: No inter-hemispheric [dgr]13CH4 trend observed, *Nature*, 486, E3-E4, 2012.

Levy, H.: Normal Atmosphere: Large Radical and Formaldehyde Concentrations Predicted, *Science*, 173, 141-143, 10.1126/science.173.3992.141, 1971.

Manning, M. R., Lowe, D. C., Moss, R. C., Bodeker, G. E., and Allan, W.: Short-term variations in the oxidizing power of the atmosphere, *Nature*, 436, 1001-1004, http://www.nature.com/nature/journal/v436/n7053/suppinfo/nature03900_S1.html, 2005.

Melton, J. R., Wania, R., Hodson, E. L., Poulter, B., Ringeval, B., Spahni, R., Bohn, T., Avis, C. A., Beerling, D. J., Chen, G., Eliseev, A. V., Denisov, S. N., Hopcroft, P. O., Lettenmaier, D. P., Riley, W. J., Singarayer, J. S., Subin, Z. M., Tian, H., Zürcher, S., Brovkin, V., van Bodegom, P. M., Kleinen, T., Yu, Z. C., and Kaplan, J. O.: Present state of global wetland extent and wetland methane modelling: conclusions from a model intercomparison project (WETCHIMP), *Biogeosciences Discuss.*, 9, 11577-11654, 10.5194/bgd-9-11577-2012, 2012.

Monteil, G., Houweling, S., Dlugockenky, E. J., Maenhout, G., Vaughn, B. H., White, J. W. C., and Rockmann, T.: Interpreting methane variations in the past two decades using measurements of CH4 mixing ratio and isotopic composition, *Atmos. Chem. Phys.*, 11, 9141-9153, 10.5194/acp-11-9141-2011, 2011.

Montzka, S. A., Spivakovsky, C. M., Butler, J. H., Elkins, J. W., Lock, L. T., and Mondeel, D. J.: New Observational Constraints for Atmospheric Hydroxyl on Global and Hemispheric Scales, *Science*, 288, 500-503, 10.1126/science.288.5465.500, 2000.

Montzka, S. A., Krol, M., Dlugokencky, E., Hall, B., Jöckel, P., and Lelieveld, J.: Small Interannual Variability of Global Atmospheric Hydroxyl, *Science*, 331, 67-69, 10.1126/science.1197640, 2011.

Morimoto, S., Aoki, S., Nakazawa, T., and Yamanouchi, T.: Temporal variations of the carbon isotopic ratio of atmospheric methane observed at Ny Ålesund, Svalbard from 1996 to 2004, *Geophysical Research Letters*, 33, L01807, 10.1029/2005GL024648, 2006.

Myhre, G., Shindell, D., Bréon, F.-M., Collins, W., Fuglestvedt, J., Huang, J., Koch, D., Lamarque, J.-F., Lee, D., Mendoza, B., Nakajima, T., Robock, A., Stephens, G., Takemura, T., and Zhang, H.: Anthropogenic and natural radiative forcing, in: Climate Change 2013: The Physical Science Basis. Contribution of Working Group I to the Fifth Assessment Report of the Intergovernmental Panel on Climate Change., edited by: T.F. Stocker, D. Q., G.-K. Plattner, M. Tignor, S.K. Allen, J. Doschung, A. Nauels, Y. Xia, V. Bex, and P.M. Midgley, Cambridge University Press, 659-740, 2013.

Naik, V., Voulgarakis, A., Fiore, A. M., Horowitz, L. W., Lamarque, J. F., Lin, M., Prather, M. J., Young, P. J., Bergmann, D., Cameron-Smith, P. J., Cionni, I., Collins, W. J., Dalsøren, S. B., Doherty, R., Eyring, V., Faluvegi, G., Folberth, G. A., Josse, B., Lee, Y. H., MacKenzie, I. A., Nagashima, T., van Noije, T. P. C., Plummer, D. A., Righi, M., Rumbold, S. T., Skeie, R., Shindell, D. T., Stevenson, D. S., Strode, S., Sudo, K., Szopa, S., and Zeng, G.: Preindustrial to present-day changes in tropospheric hydroxyl radical and methane lifetime from the Atmospheric Chemistry and Climate Model Intercomparison Project (ACCMIP), *Atmos. Chem. Phys.*, 13, 5277-5298, 10.5194/acp-13-5277-2013, 2013.

Neef, L., van Weele, M., and van Velthoven, P.: Optimal estimation of the present-day global methane budget, *Global Biogeochem. Cycles*, 24, GB4024, 10.1029/2009GB003661, 2010.

Nisbet, E. G., Dlugokencky, E. J., and Bousquet, P.: Methane on the Rise—Again, *Science*, 343, 493-495, 10.1126/science.1247828, 2014.

O'Connor, F. M., Boucher, O., Gedney, N., Jones, C. D., Folberth, G. A., Coppell, R., Friedlingstein, P., Collins, W. J., Chappellaz, J., Ridley, J., and Johnson, C. E.: Possible role of wetlands, permafrost, and methane hydrates in the methane cycle under future climate change: A review, *Rev. Geophys.*, 48, n/a-n/a, 10.1029/2010RG000326, 2010.

Patra, P. K., Krol, M. C., Montzka, S. A., Arnold, T., Atlas, E. L., Lintner, B. R., Stephens, B. B., Xiang, B., Elkins, J. W., Fraser, P. J., Ghosh, A., Hintsa, E. J., Hurst, D. F., Ishijima, K., Krummel, P. B., Miller, B. R., Miyazaki, K., Moore, F. L., Muhle, J., O/'Doherty, S., Prinn, R. G., Steele, L. P., Takigawa, M., Wang, H. J., Weiss, R. F., Wofsy, S. C., and Young, D.: Observational evidence for interhemispheric hydroxyl-radical parity, *Nature*, 513, 219-223, 10.1038/nature13721, 2014.

Pison, I., Bousquet, P., Chevallier, F., Szopa, S., and Hauglustaine, D.: Multi-species inversion of CH4, CO and H2 emissions from surface measurements, *Atmos. Chem. Phys.*, 9, 5281-5297, 10.5194/acp-9-5281-2009, 2009.

Pison, I., Ringeval, B., Bousquet, P., Prigent, C., and Papa, F.: Stable atmospheric methane in the 2000s: key-role of emissions from natural wetlands, *Atmos. Chem. Phys.*, 13, 11609-11623, 10.5194/acp-13-11609-2013, 2013.

Prinn, R. G., Huang, J., Weiss, R. F., Cunnold, D. M., Fraser, P. J., Simmonds, P. G., McCulloch, A., Harth, C., Salameh, P., O'Doherty, S., Wang, R. H. J., Porter, L., and Miller, B. R.: Evidence for Substantial Variations of Atmospheric Hydroxyl Radicals in the Past Two Decades, *Science*, 292, 1882-1888, 10.1126/science.1058673, 2001.

Prinn, R. G., Huang, J., Weiss, R. F., Cunnold, D. M., Fraser, P. J., Simmonds, P. G., McCulloch, A., Harth, C., Reimann, S., Salameh, P., O'Doherty, S., Wang, R. H. J., Porter, L. W., Miller, B. R., and Krummel, P. B.: Evidence for variability of atmospheric hydroxyl radicals over the past quarter century, *Geophysical Research Letters*, 32, L07809, 10.1029/2004GL022228, 2005.

Rigby, M., Prinn, R. G., Fraser, P. J., Simmonds, P. G., Langenfelds, R. L., Huang, J., Cunnold, D. M., Steele, L. P., Krummel, P. B., Weiss, R. F., O'Doherty, S., Salameh, P. K., Wang, H. J., Harth, C. M., Mühle, J., and Porter, L. W.: Renewed growth of atmospheric methane, *Geophysical Research Letters*, 35, L22805, 10.1029/2008GL036037, 2008.

Rohrer, F., and Berresheim, H.: Strong correlation between levels of tropospheric hydroxyl radicals and solar ultraviolet radiation, *Nature*, 442, 184-187, http://www.nature.com/nature/journal/v442/n7099/suppinfo/nature04924_S1.html, 2006.

Schultz, M., van het Bolscher, M., Pulles, T., Brand, R., Pereira, J., Spessa, A., Dalsøren, S., van Nojie, T., Szopa, S., and Schultz, M.: Emission data sets and methodologies for estimating emissions.REanalysis of the TROpospheric chemical composition over the past 40 years. A long-term global modeling study of tropospheric chemistry funded under the 5th EU framework programme. EU-Contract No. EVK2-CT-2002-00170 2008.

Schwietzke, S., Griffin, W. M., Matthews, H. S., and Bruhwiler, L. M. P.: Global Bottom-Up Fossil Fuel Fugitive Methane and Ethane Emissions Inventory for Atmospheric Modeling, *ACS Sustainable Chemistry & Engineering*, 2, 1992-2001, 10.1021/sc500163h, 2014.

Simpson, I. J., Chen, T.-Y., Blake, D. R., and Rowland, F. S.: Implications of the recent fluctuations in the growth rate of tropospheric methane, *Geophysical Research Letters*, 29, 117-111-117-114, 10.1029/2001GL014521, 2002.

Simpson, I. J., Rowland, F. S., Meinardi, S., and Blake, D. R.: Influence of biomass burning during recent fluctuations in the slow growth of global tropospheric methane, *Geophysical Research Letters*, 33, L22808, 10.1029/2006GL027330, 2006.

Simpson, I. J., Sulbaek Andersen, M. P., Meinardi, S., Bruhwiler, L., Blake, N. J., Helmig, D., Rowland, F. S., and Blake, D. R.: Long-term decline of global atmospheric ethane concentrations and implications for methane, *Nature*, 488, 490-494, http://www.nature.com/nature/journal/v488/n7412/abs/nature11342.html#supplementary-information, 2012.

Sindelarova, K., Granier, C., Bouarar, I., Guenther, A., Tilmes, S., Stavrakou, T., Müller, J. F., Kuhn, U., Stefani, P., and Knorr, W.: Global dataset of biogenic VOC emissions calculated by the MEGAN model over the last 30 years, *Atmos. Chem. Phys. Discuss.*, 14, 10725-10788, 10.5194/acpd-14-10725-2014, 2014.

Spahni, R., Wania, R., Neef, L., van Weele, M., Pison, I., Bousquet, P., Frankenberg, C., Foster, P. N., Joos, F., Prentice, I. C., and van Velthoven, P.: Constraining global methane emissions and uptake by ecosystems, *Biogeosciences*, 8, 1643-1665, 10.5194/bg-8-1643-2011, 2011.

Strode, S. A., Duncan, B. N., Yegorova, E. A., Kouatchou, J., Ziemke, J. R., and Douglass, A. R.: Implications of carbon monoxide bias for methane lifetime and atmospheric composition in chemistry climate models, *Atmos. Chem. Phys.*, 15, 11789-11805, 10.5194/acp-15-11789-2015, 2015.

Sussmann, R., Forster, F., Rettinger, M., and Bousquet, P.: Renewed methane increase for five years (2007–2011) observed by solar FTIR spectrometry, *Atmos. Chem. Phys.*, 12, 4885-4891, 10.5194/acp-12-4885-2012, 2012.

Søvde, O. A., Prather, M. J., Isaksen, I. S. A., Berntsen, T. K., Stordal, F., Zhu, X., Holmes, C. D., and Hsu, J.: The chemical transport model Oslo CTM3, *Geosci. Model Dev.*, 5, 1441-1469, 10.5194/gmd-5-1441-2012, 2012.

Tsutsumi, Y., Kazumasa, M., Takatoshi, H., Masaaki, I., and Conway, T. J.: Technical Report of Global Analysis Method for Major Greenhouse Gases by the World Data Center for Greenhouse Gases, WMO, 2009.

van der Werf, G. R., Randerson, J. T., Giglio, L., Collatz, G. J., Mu, M., Kasibhatla, P. S., Morton, D. C., DeFries, R. S., Jin, Y., and van Leeuwen, T. T.: Global fire emissions and the contribution of deforestation, savanna, forest, agricultural, and peat fires (1997–2009), *Atmos. Chem. Phys.*, 10, 11707-11735, 10.5194/acp-10-11707-2010, 2010.

Wang, J. S., Logan, J. A., McElroy, M. B., Duncan, B. N., Megretskaia, I. A., and Yantosca, R. M.: A 3-D model analysis of the slowdown and interannual variability in the methane growth rate from 1988 to 1997, *Global Biogeochem. Cycles*, 18, GB3011, 10.1029/2003GB002180, 2004.

Wang, J. S., McElroy, M. B., Logan, J. A., Palmer, P. I., Chameides, W. L., Wang, Y., and Megretskaia, I. A.: A quantitative assessment of uncertainties affecting estimates of global mean OH derived from methyl chloroform observations, *Journal of Geophysical Research: Atmospheres*, 113, D12302, 10.1029/2007JD008496, 2008.

Warwick, N. J., Bekki, S., Law, K. S., Nisbet, E. G., and Pyle, J. A.: The impact of meteorology on the interannual growth rate of atmospheric methane, *Geophysical Research Letters*, 29, 1947, 10.1029/2002GL015282, 2002.

West, J. J., and Fiore, A. M.: Management of Tropospheric Ozone by Reducing Methane Emissions, *Environ. Sci. Technol.*, 39, 4685-4691, 10.1021/es048629f, 2005.

Worden, J., Jiang, Z., Jones, D. B. A., Alvarado, M., Bowman, K., Frankenberg, C., Kort, E. A., Kulawik, S. S., Lee, M., Liu, J., Payne, V., Wecht, K., and Worden, H.: El Niño, the 2006 Indonesian peat fires, and the distribution of atmospheric methane, *Geophysical Research Letters*, 40, 4938-4943, 10.1002/grl.50937, 2013.

Table 1. Overview of simulations performed with the Oslo CTM3 model.

Simulation name	Period	Characteristics	Difference from main simulation
Main	1970-Oct 2012	Standard emissions described in section 2.1.1. Meteorology described in this section.	
Fixed methane	1970-Oct 2012		*No prescription of methane emissions*. Surface methane levels kept fixed. Monthly mean 1970 levels used repeatedly for all years
Fixed meteorology	1997-Oct 2012		*Year 2001 meteorology*
Financial*	2009-Oct 2012		*Alternative extrapolation* of anthropogenic emissions to account for the *financial crisis*
Bio*	1980-2012		*Inter-annual variation* in *biogenic* emissions of NMVOCs and CO

*Results (and setup) from these simulations are mainly discussed in the Supplement.

Table 2. Coefficient of determination (R^2) between <CH4 model> – [<CH4 model>] and <Total tracer> - [<Total tracer>] for stations shown in Fig. 5-10. Parameters for equation 1 and RMSE for a linear fit between <CH4 model> – [<CH4 model>] and <Total tracer> - [<Total tracer>].

Station	**Figure**	**R^2 between <CH4 model> – [<CH4 model>] and <Total tracer> - [<Total tracer>]**	**Residual**	**B**	**RMSE**
Ascension Island	6a	0.80	-3.01	1.21	0.74
Tutuila	6b	0.87	5.08	1.49	0.82
Cape Grim	6c	0.98	-0.15	0.97	0.05
Ushuaia	6d	0.83	-0.27	0.94	0.09
Alert	7a	0.69	-2.16	1.66	0.85
Wendover	7b	0.54	-5.74	0.78	1.07
Key Biscayne	7c	0.95	6.10	1.38	1.40
Mauna Loa	7d	0.87	18.41	1.80	1.27
Zeppelinfjellet	8a	0.91	-1.67	1.13	0.59
Pallas-Sammaltun	8b	0.95	-3.38	1.18	0.75
Mace Head	8c	0.97	-3.28	1.16	0.56
Hegyhatsal	8d	1.00	-2.46	1.15	0.96
Sede Boker	9a	0.83	5.41	1.23	0.97
Ulaan Uul	9b	0.95	1.15	1.10	0.65
Sary Taukum	9c	0.97	-8.27	1.11	0.96
Tae-ahn Peninsula	9d	0.97	0.77	1.07	1.15
Cape Rama	10a	0.92	-9.60	1.24	1.02
Mahe Island	10b	0.85	6.68	1.42	1.22

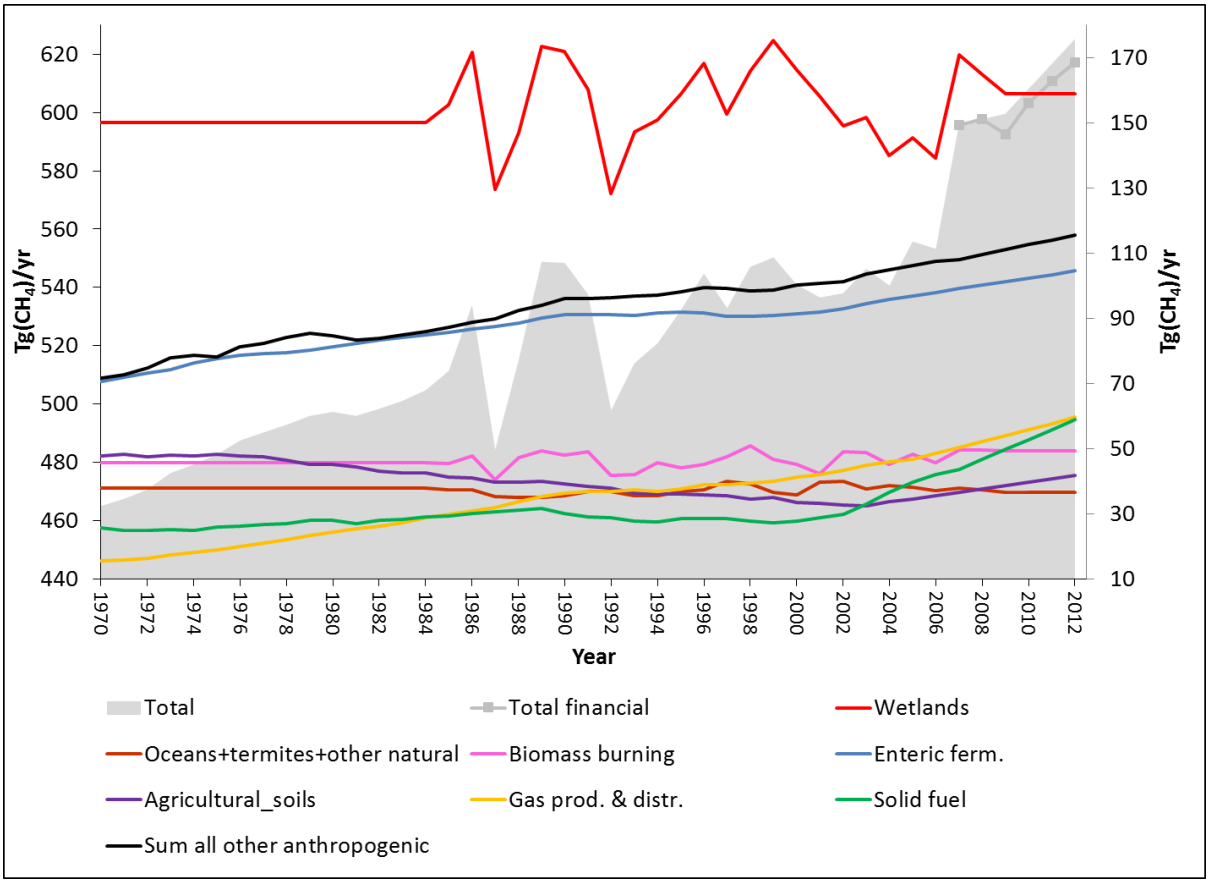

Figure 1. Emissions used in the model simulations. The grey shaded area is the total CH_4 emissions (left y-axis). The total emissions in the alternative extrapolation accounting for the financial crisis are shown from 2006 and onwards as the grey line with markers. The other colored lines are the CH_4 emissions from the main emission sectors (right y-axis).

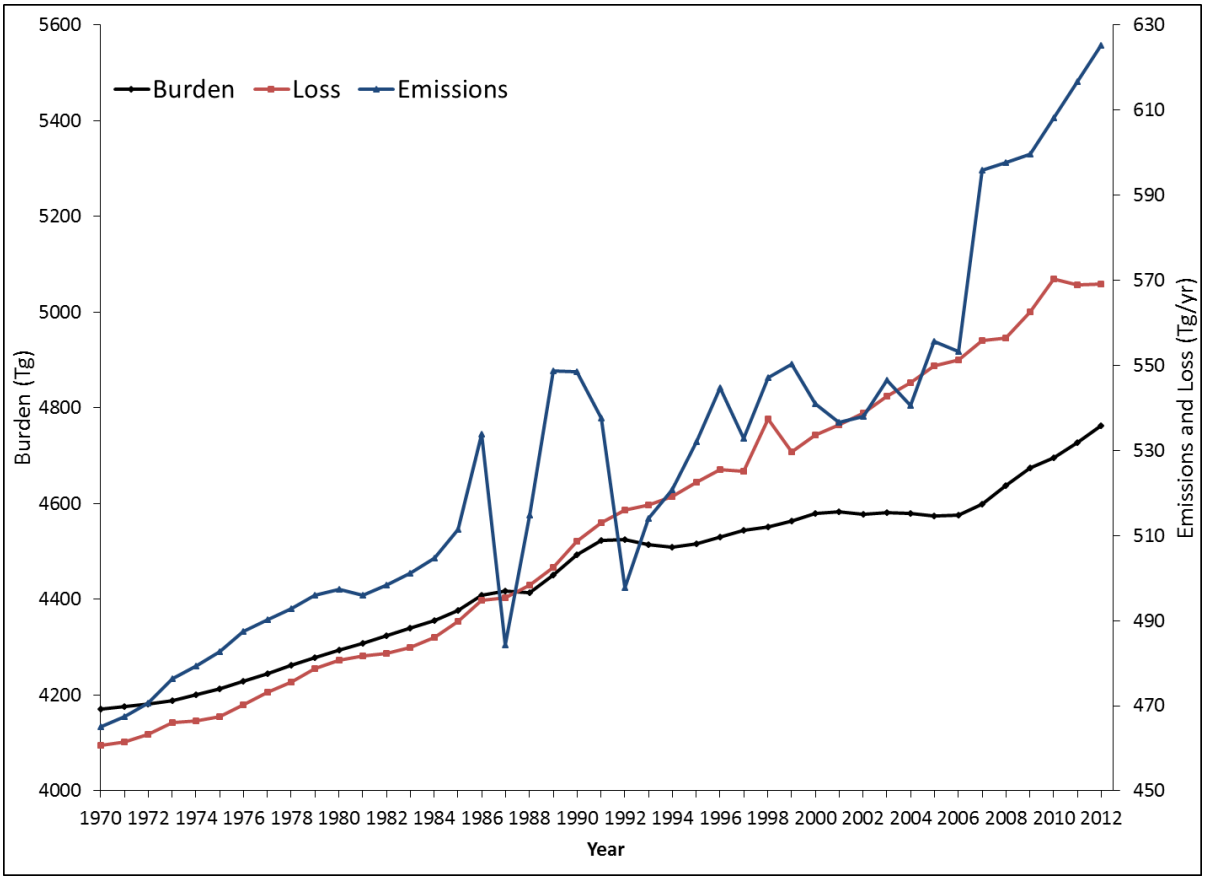

Figure 2. Global CH_4 budget in the main Oslo CTM3 simulation over the period 1970-2012: Atmospheric burden (left y-axis), loss: atmospheric chemical destruction + soil uptake (right y-axis), and total emissions (right y-axis).

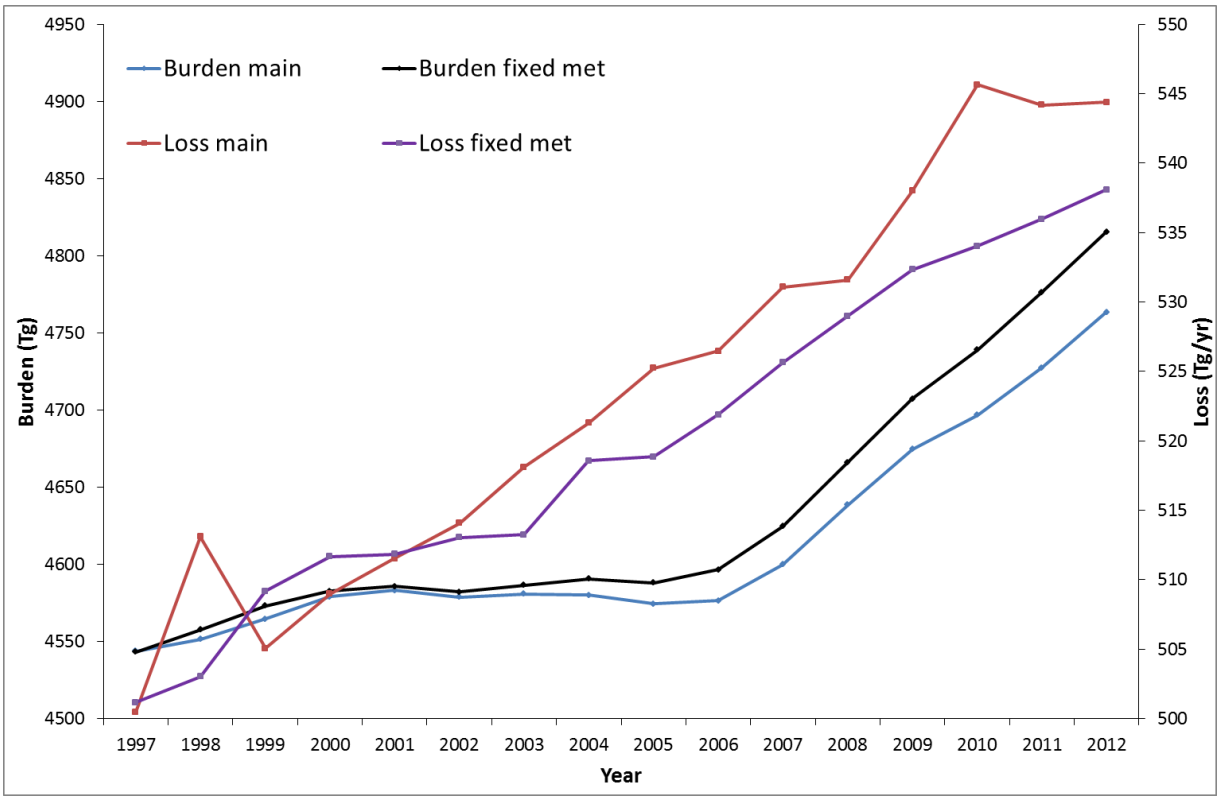

Figure 3. Atmospheric CH_4 burden and atmospheric chemical loss for the simulation with "fixed meteorology" and the "main" simulation.

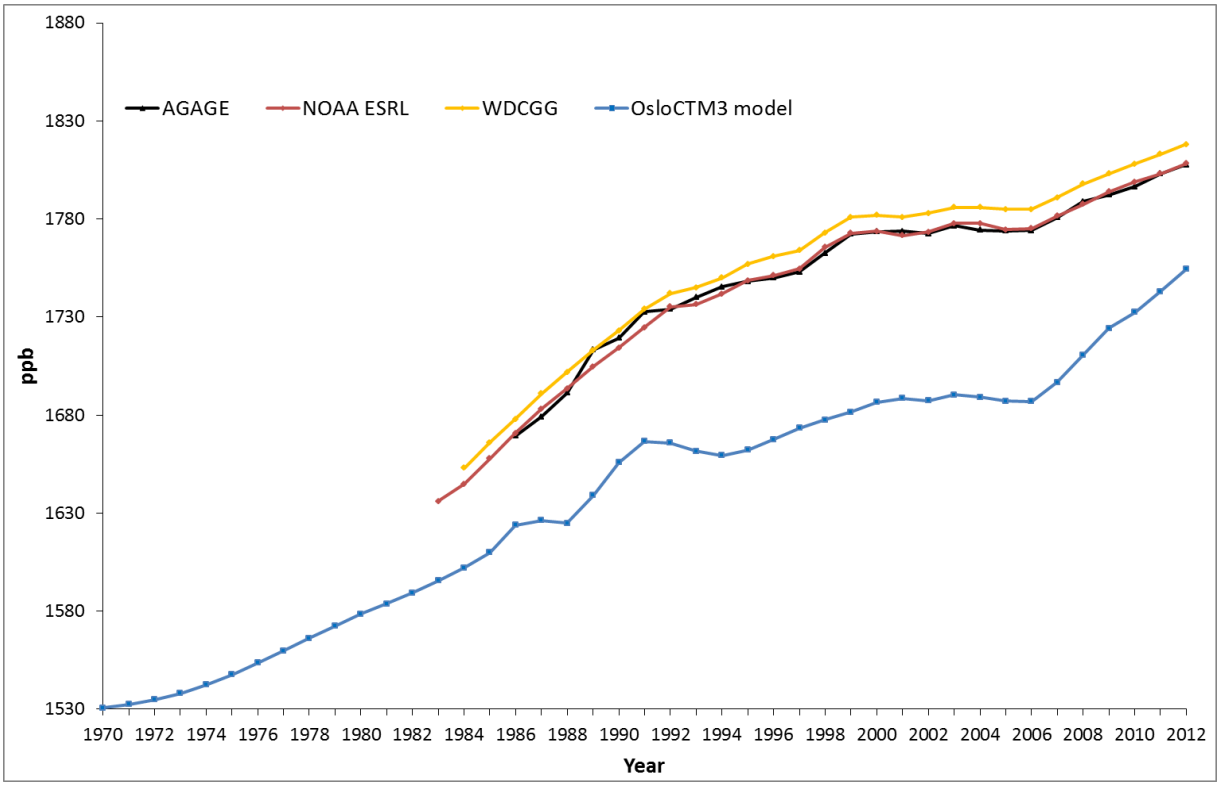

Figure 4. Global mean surface CH_4 mixing ratio in the main model simulation compared to global mean surface CH_4 mixing ratio calculated from the global networks AGAGE (http://agage.eas.gatech.edu/data_archive/global_mean/global_mean_md.txt), NOAA ESRL (http://www.esrl.noaa.gov/gmd/ccgg/mbl/data.php), and WDCGG (http://ds.data.jma.go.jp/gmd/wdcgg/pub/global/globalmean.html).

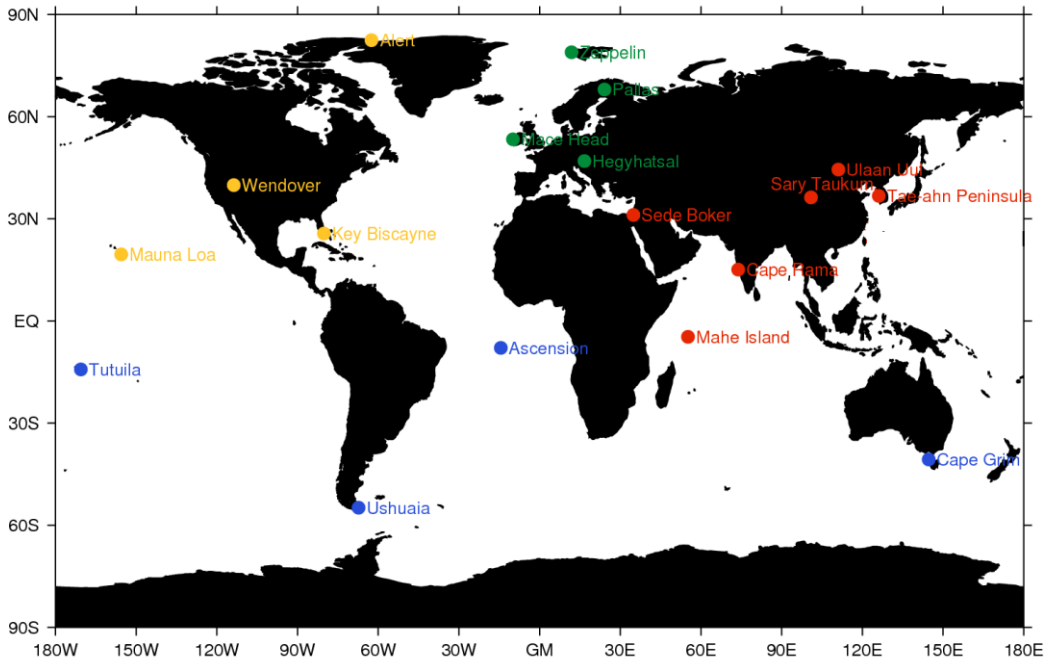

Figure 5. Location of the 18 surface stations used in comparison between measurements and model in this section. Blue: Stations in the Southern Hemisphere, orange: Stations in or near North America, green: stations in or near Europe, red: stations in or near Asia.

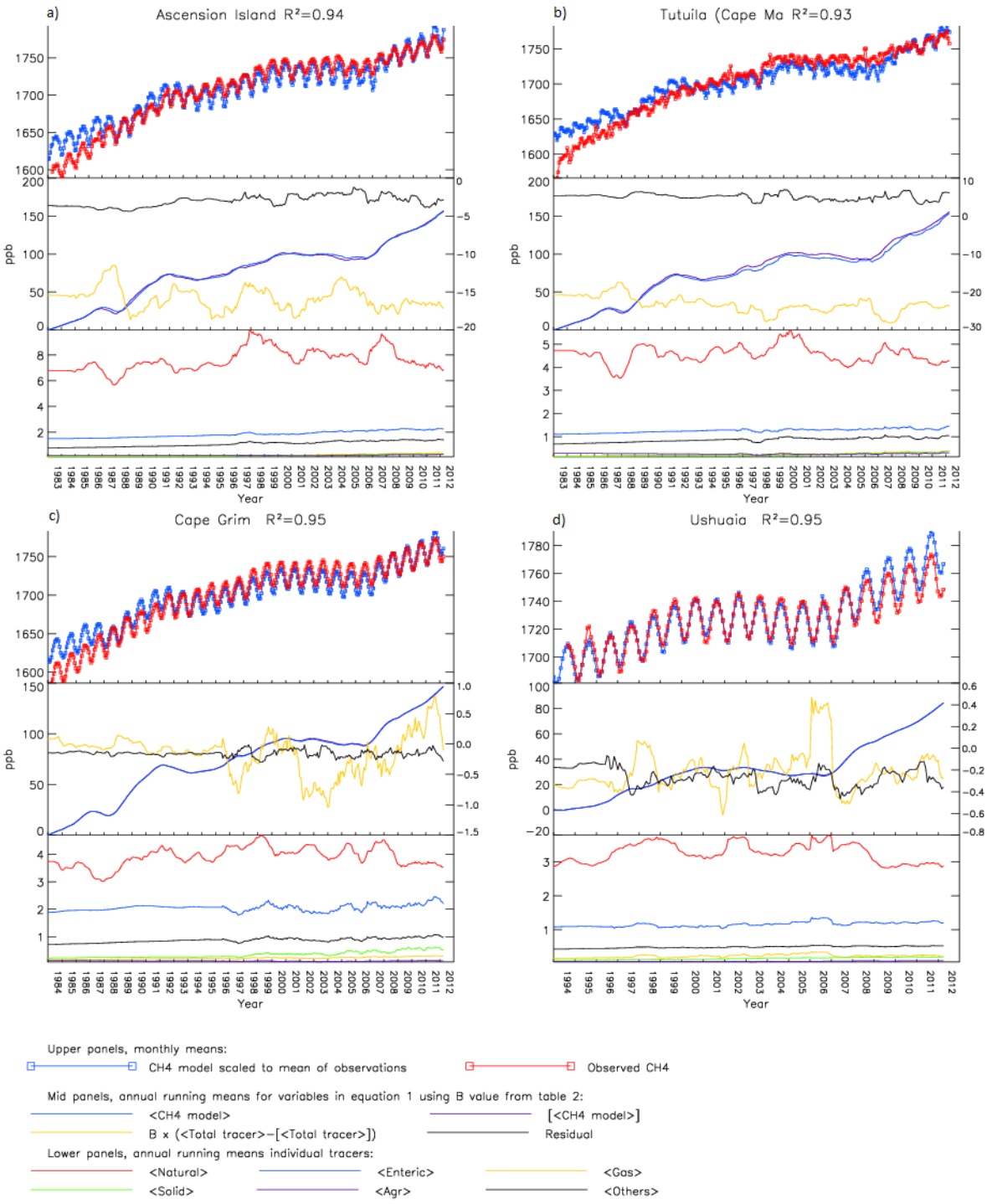

Figure 6. Evolution of CH_4 and tracers at stations (a: Ascension Island, b: Tutuila, c: Cape Grim, d: Ushuaia) in the Southern Hemisphere. Upper panel in each figure: Comparison of monthly mean surface CH_4 in model and observations. The model results are scaled to the observed mean CH_4 level over the periods of measurements. Mid panels: Variables from equation 1. <> denotes annual running mean, [ ] denotes longitudinal mean. Left y-axis: <CH_4 model> and [<CH_4 model>] are scaled down to be initialized to zero in the first year. Right y-

axis: B x (<Total tracer>-[<Total tracer>]) and Residual. Lower panels: Evolution of various emission tracers, see Table S1 in the Supplement for detailed information.

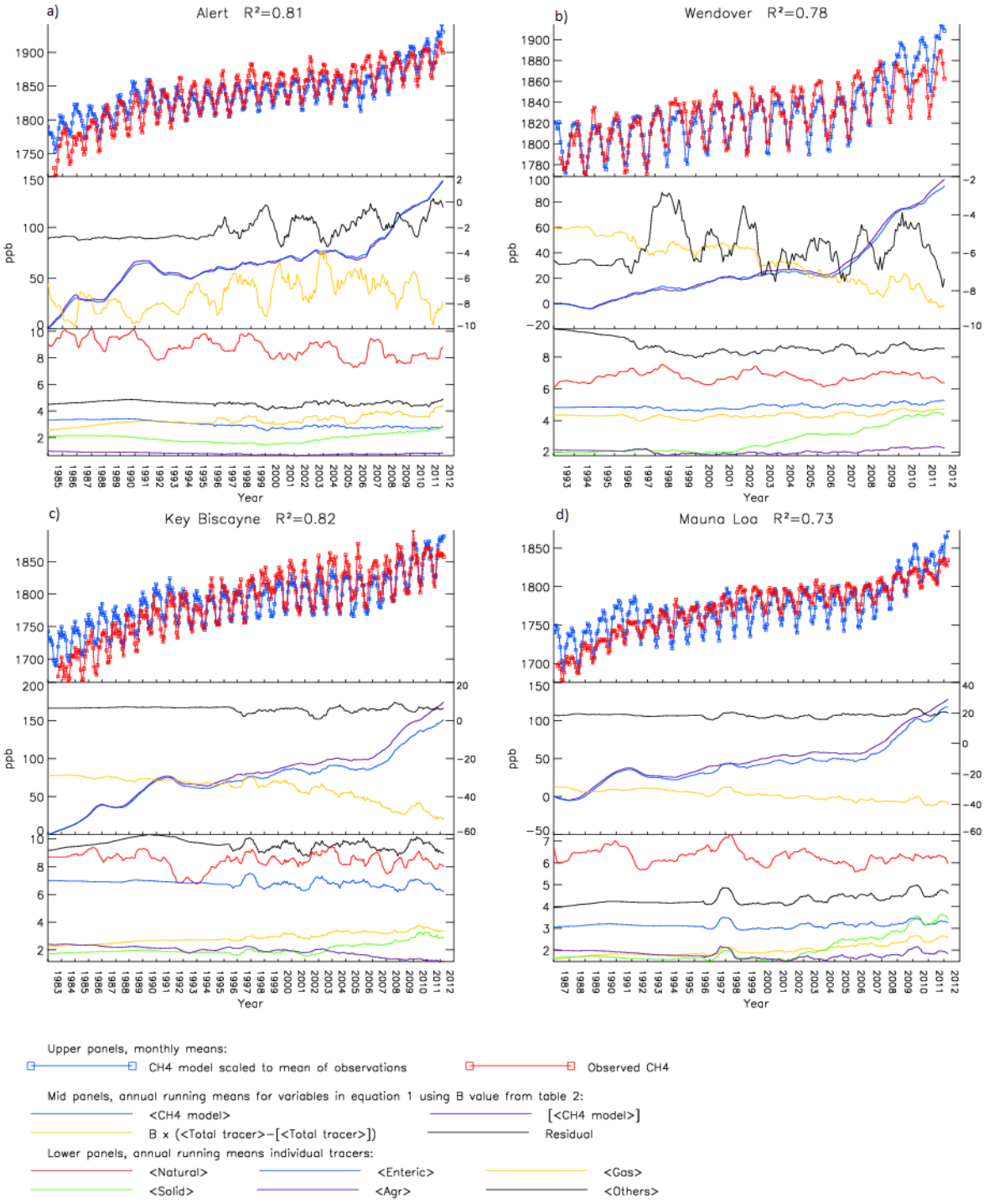

Figure 7. Evolution of CH_4 and tracers at stations (a: Alert, b: Wendover, c: Key Biscayne, d: Mauna Loa) in or near North America. See Fig. 6 caption for further description.

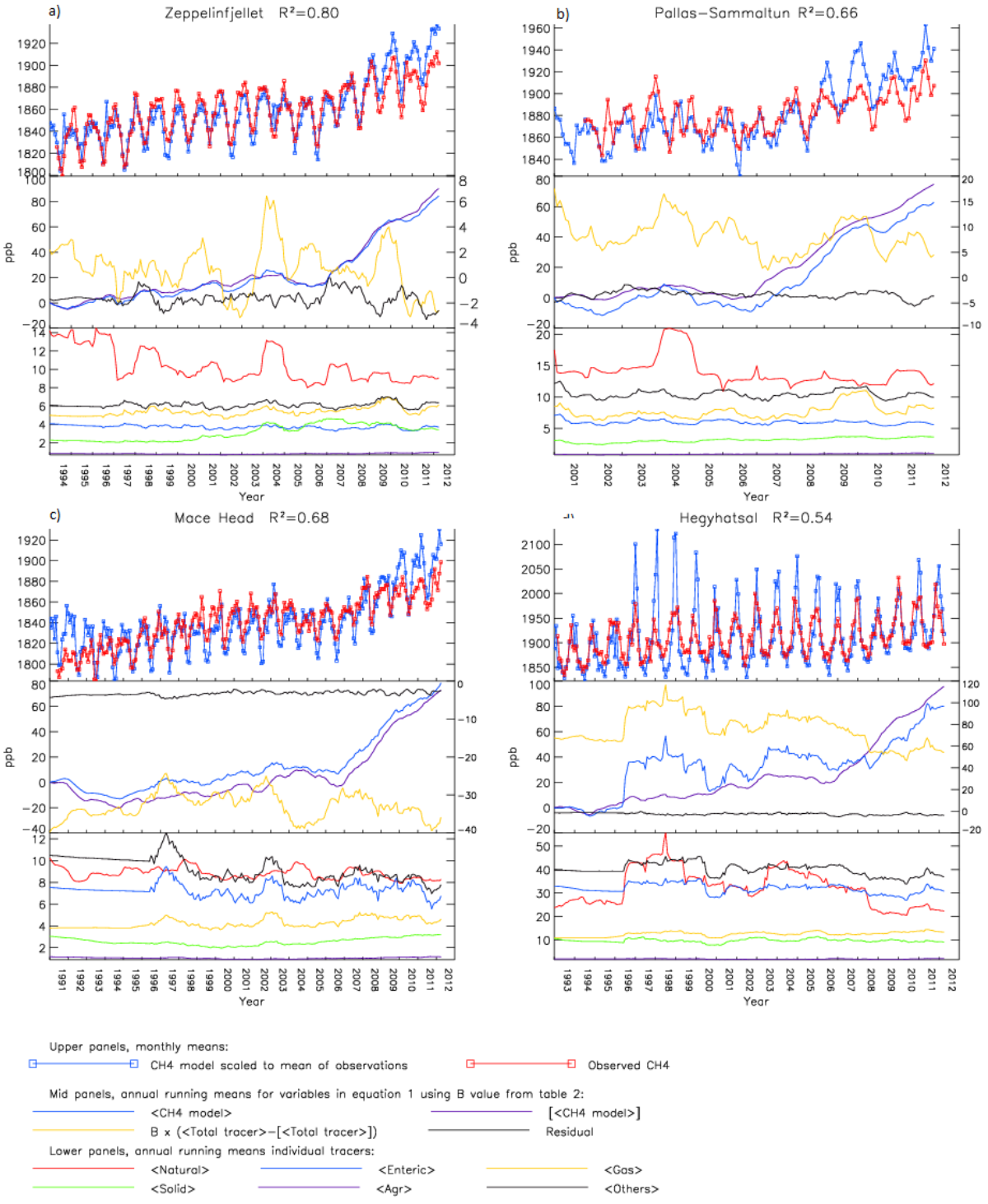

Figure 8. Evolution of CH_4 and tracers at stations (a: Zeppelinfjellet, b: Pallas-Sammaltun, c: Mace Head, d: Hegyhatsal) in or near Europe. See Fig. 6 caption for further description.

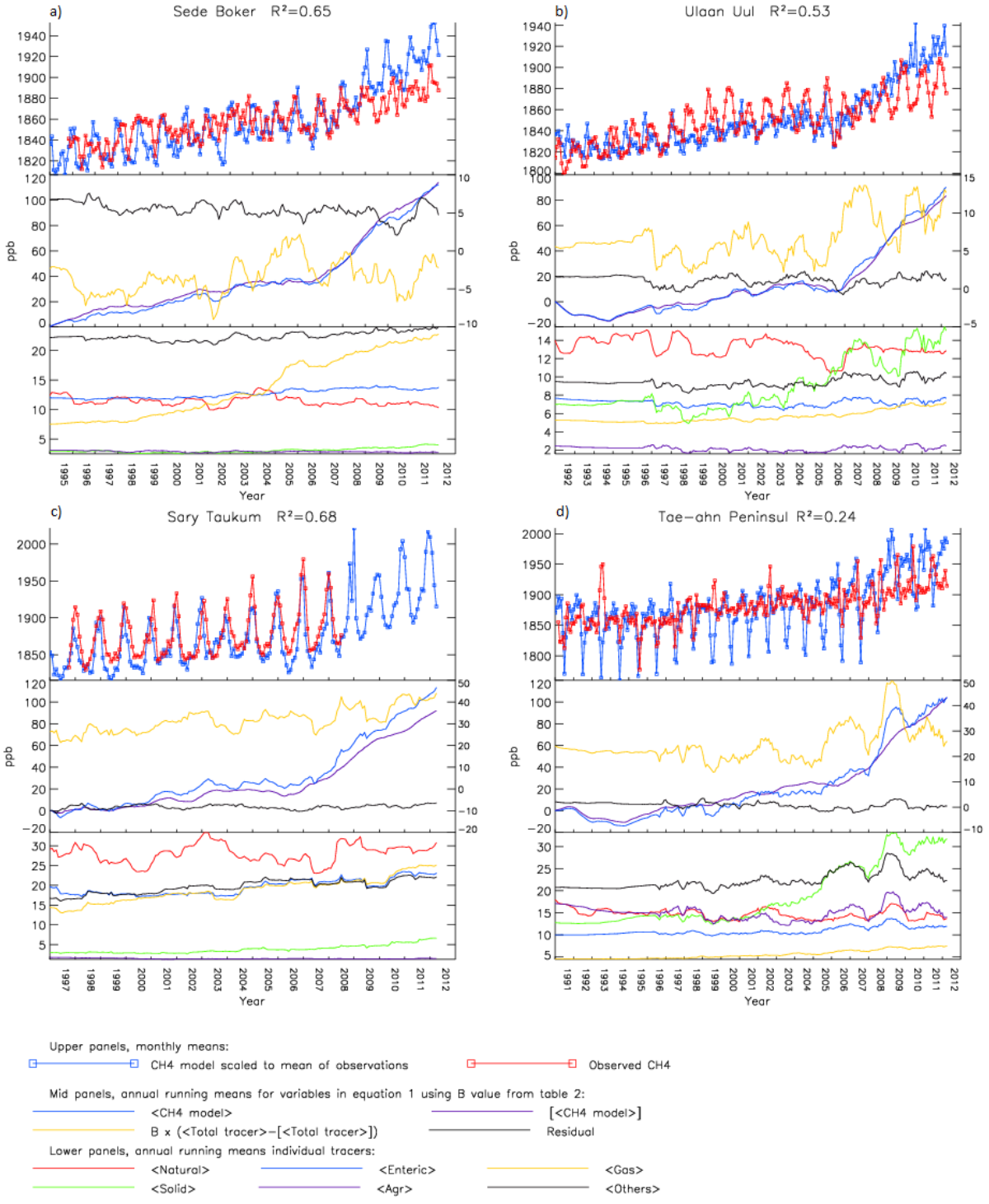

Figure 9. Evolution of CH_4 and tracers at stations (a: Sede Boker, b: Ulaan Uul, c: Sary Taukum, d: Tae-ahn Peninsula) near Asian emission sources. See Fig. 6 caption for further description.

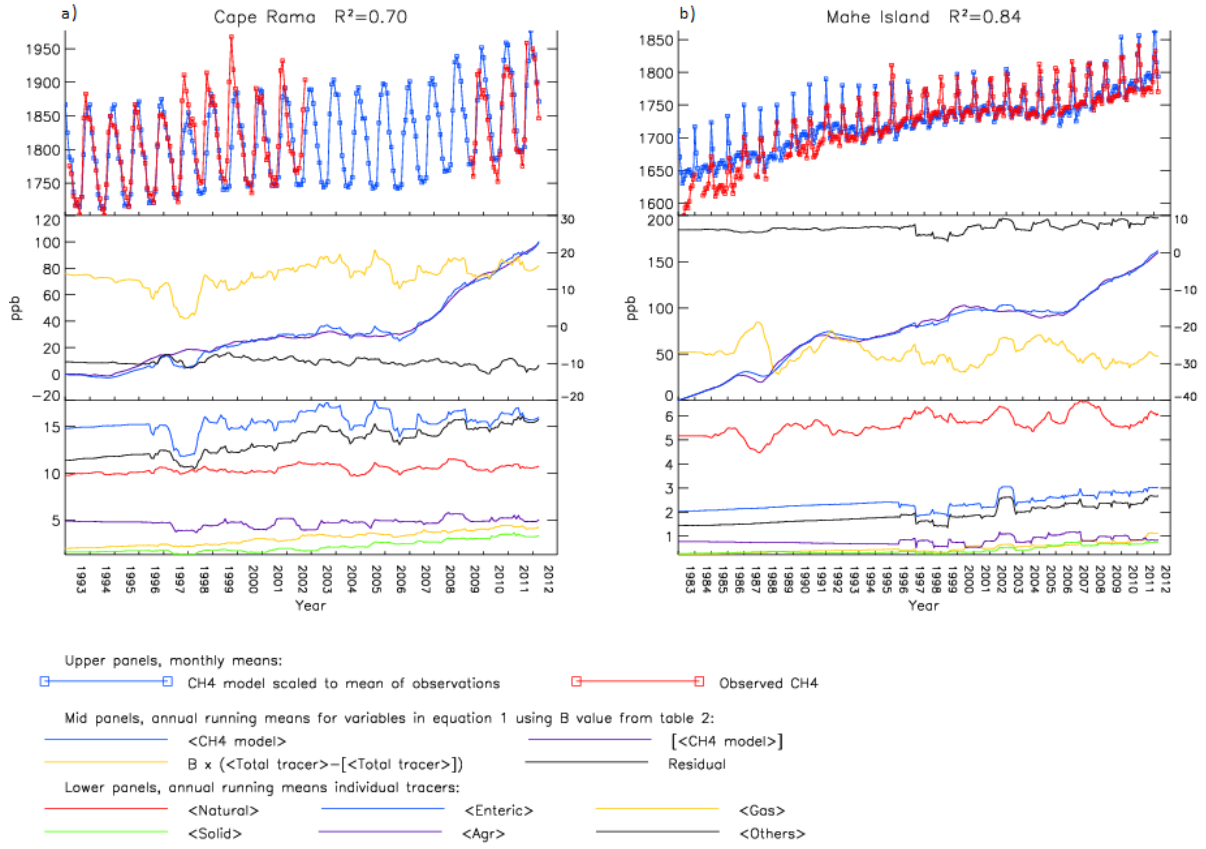

Figure 10. Evolution of CH_4 and tracers at stations (: a: Cape Rama, b: Mahe Island) in background/outflowing air in or near Asia. See Fig. 6 caption for further description.

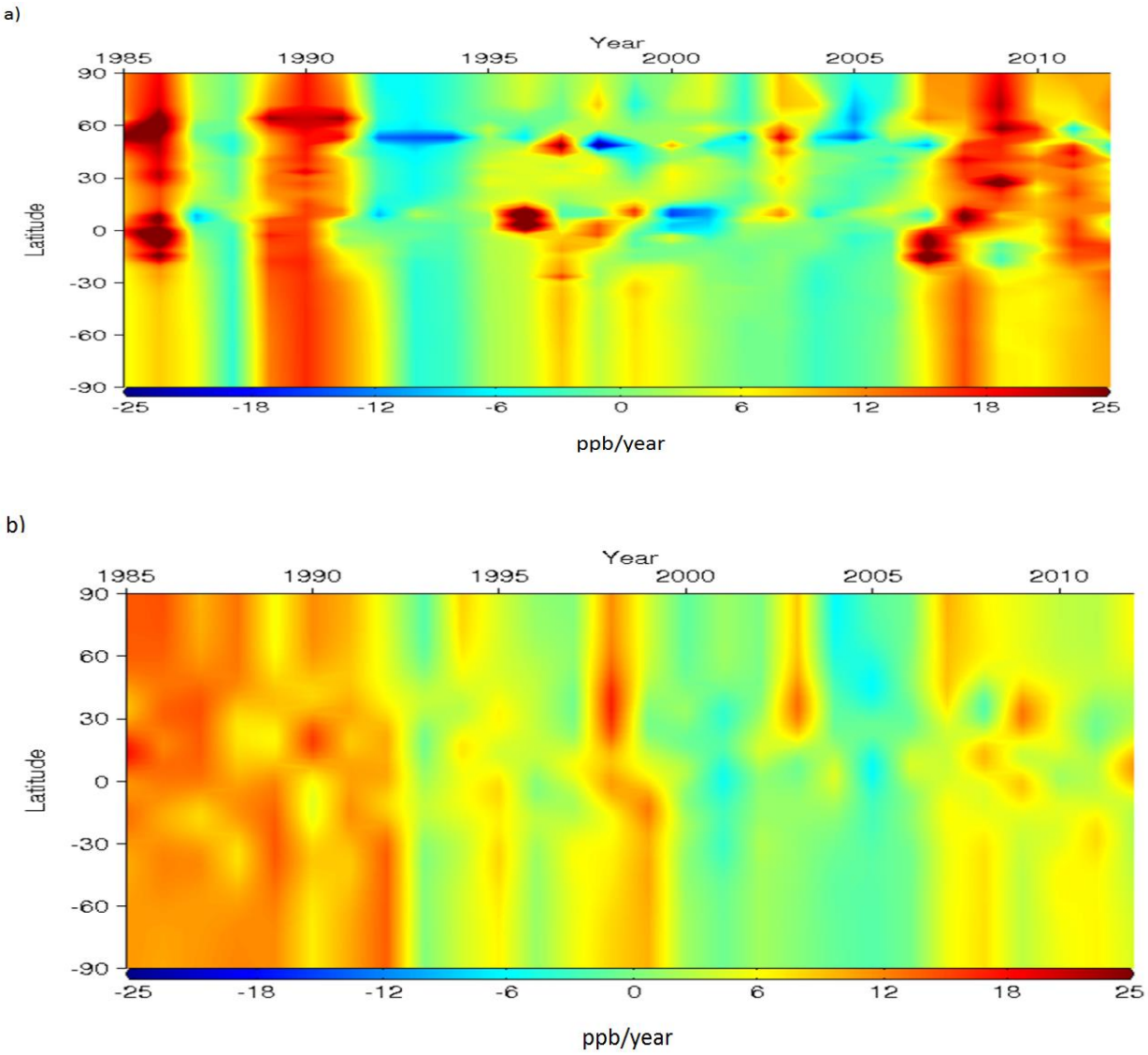

Figure 11. CH_4 year to year variation (ppb) in surface CH_4 in model (Plot a) compared to the levels of surface CH_4 estimated from observations (Plot b) in various latitudinal bands based on the NOAA ESRL network of surface stations (Ciais et al. 2013, and data set provided by Edward J. Dlugokencky: private communication).

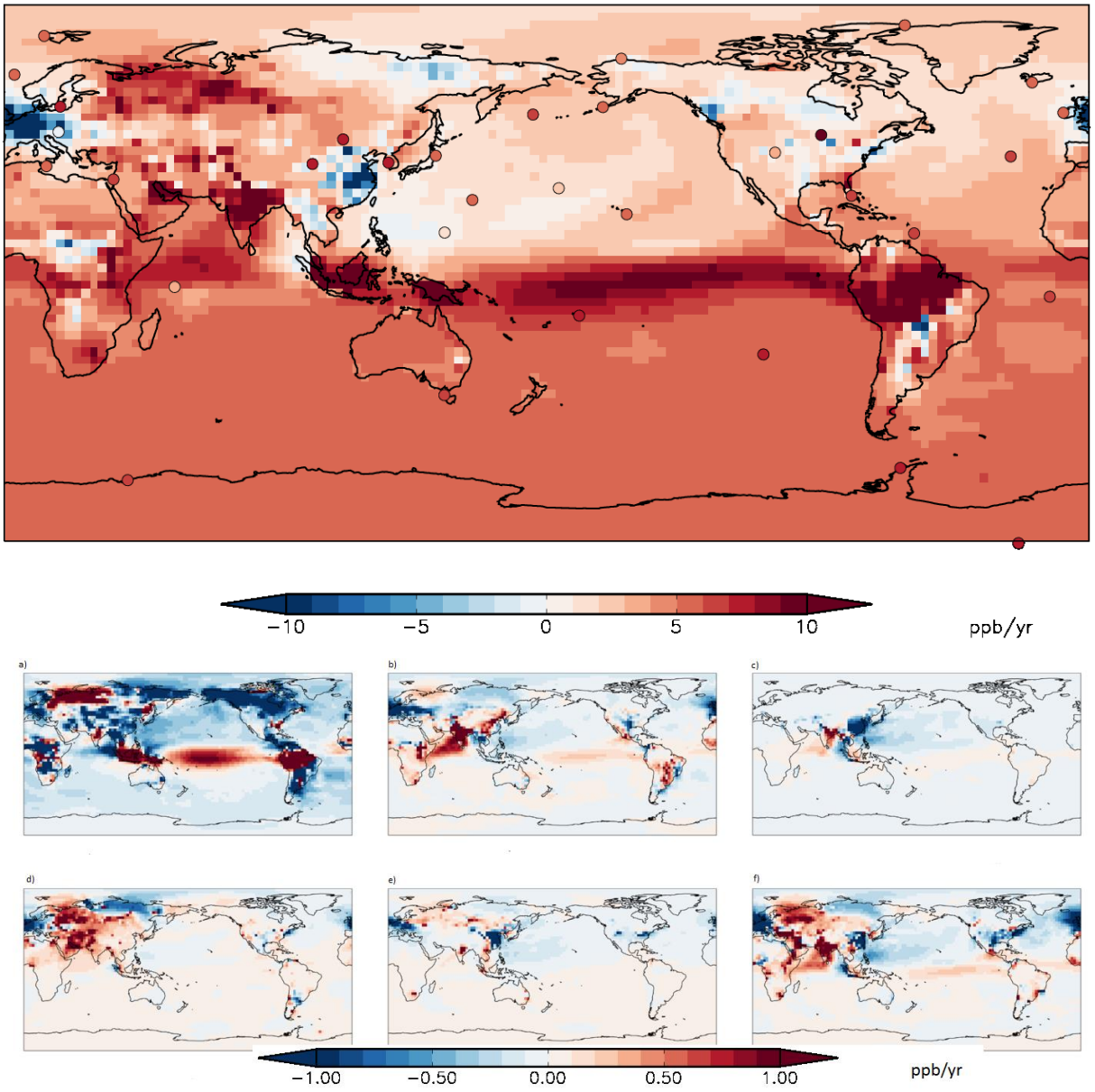

Figure 12. Upper panel: Mean year-to-year growth (ppb/yr) in surface CH_4 in Oslo CTM3 over the period 1998-2000. The 32 circles show the observed growth rates over the same period. The stations picked for comparison is based on the criteria described in section 2.3, and only observation sites that have measurements available for all months within the given time is included. Panels a)-f): Mean year-to-year growth ppb/yr) of emission tracers in the same period. a) Natural (wetlands+other natural+biomass burning), b) enteric, c) agricultural soils, d) gas, e) solid fuel, f) sum all other anthropogenic tracers.

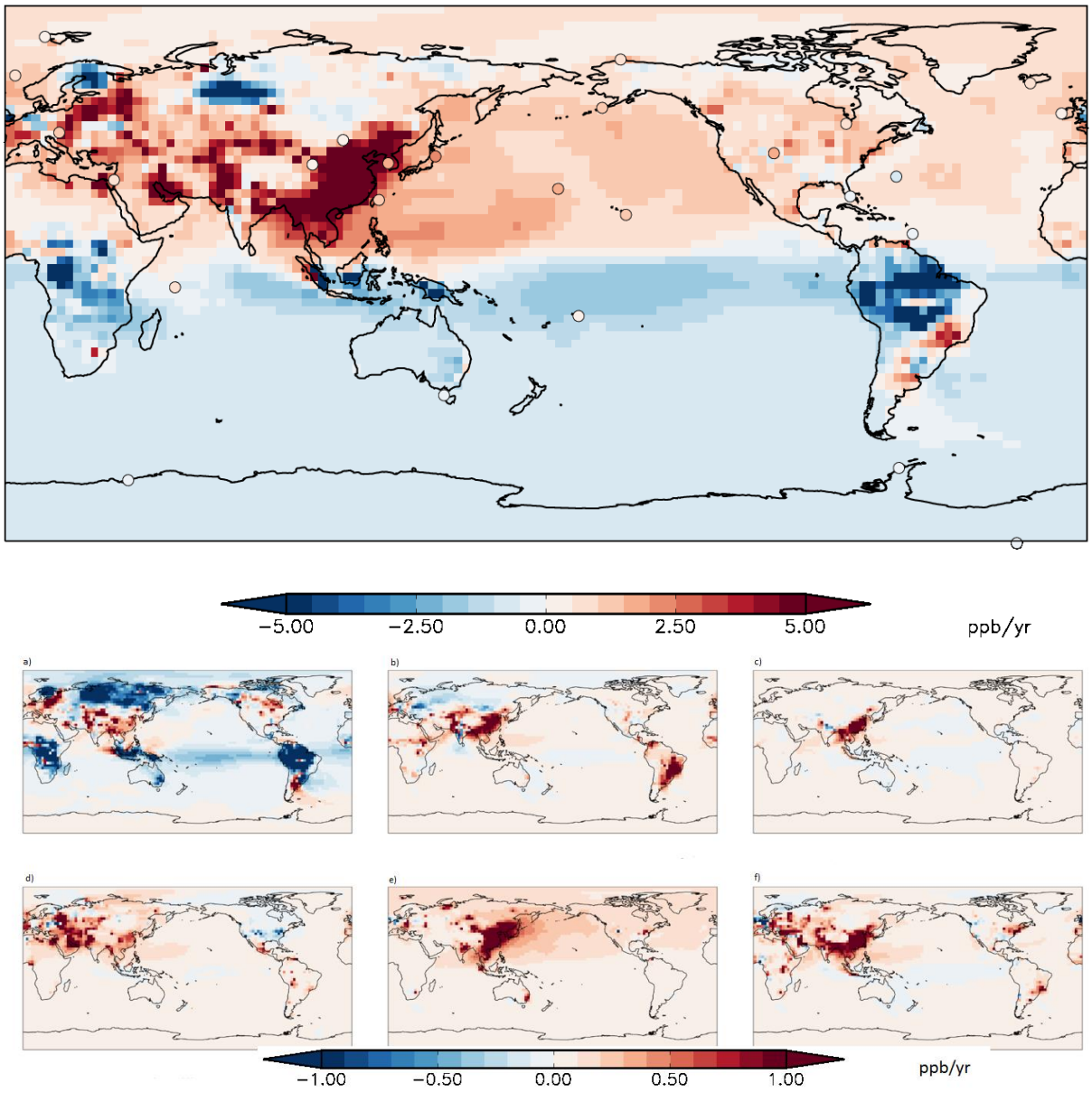

Figure 13. Upper panel: Mean year-to-year growth (ppb/yr) in surface CH_4 in Oslo CTM3 over the period 2001-2006. The 25 circles show the observed growth rates over the same period. The stations picked for comparison is based on the criteria described in section 2.3, and only observation sites that have measurements available for all months within the given time is included. Panels a)-f): Mean year-to-year growth (ppb/yr) of emission tracers in the same period. a) Natural (wetlands+other natural+biomass burning), b) enteric, c) agricultural soils, d) gas, e) solid fuel, f) sum all other anthropogenic tracers.

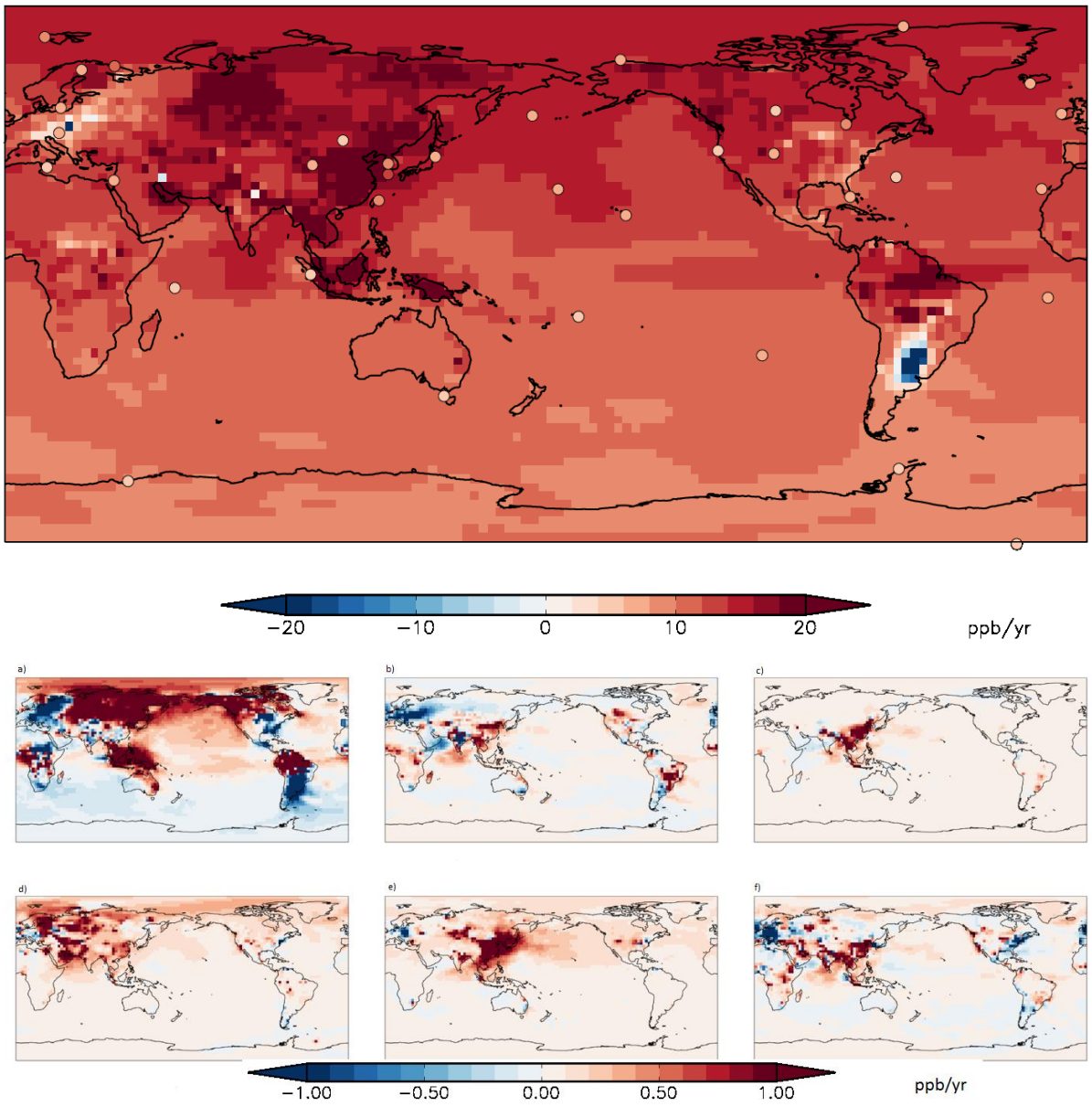

Figure 14. Upper panel: Mean year-to-year growth (ppb/yr) in surface CH_4 in Oslo CTM3 over the period 2007-2009. The 36 circles show the observed growth rates over the same period. The stations picked for comparison are based on the criteria described in section 2.3, and only observation sites that have measurements available for all months within the given time is included. Panels a)-f): Mean year-to-year growth (ppb/yr) in mole fraction of emission tracers in the same period. a) Natural (wetlands+other natural+biomass burning), b) enteric, c) agricultural soils, d) gas, e) solid fuel, f) sum all other anthropogenic tracers.

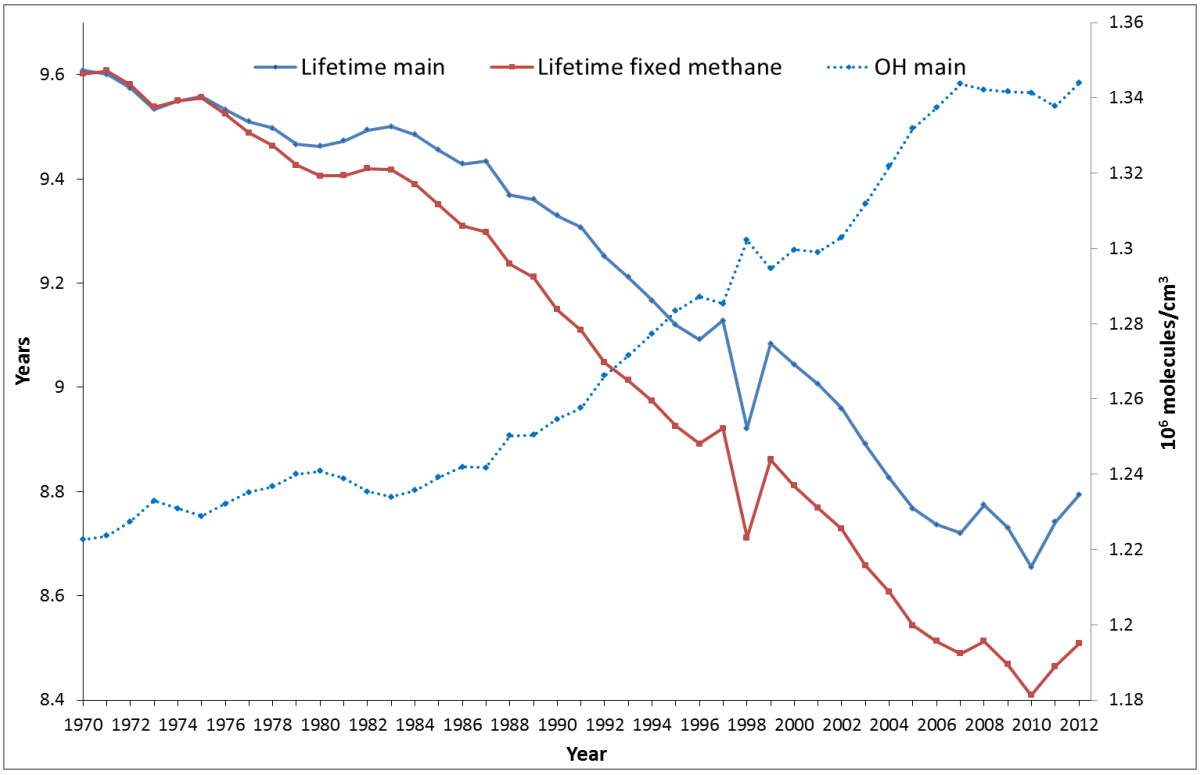

Figure 15. Evolution of yearly global average atmospheric instantaneous CH_4 lifetime in the main and fixed methane simulations (left y-axis). Evolution of yearly global average atmospheric OH concentration in the main simulation (right y-axis) using the reaction rate with CH_4 as averaging kernel.

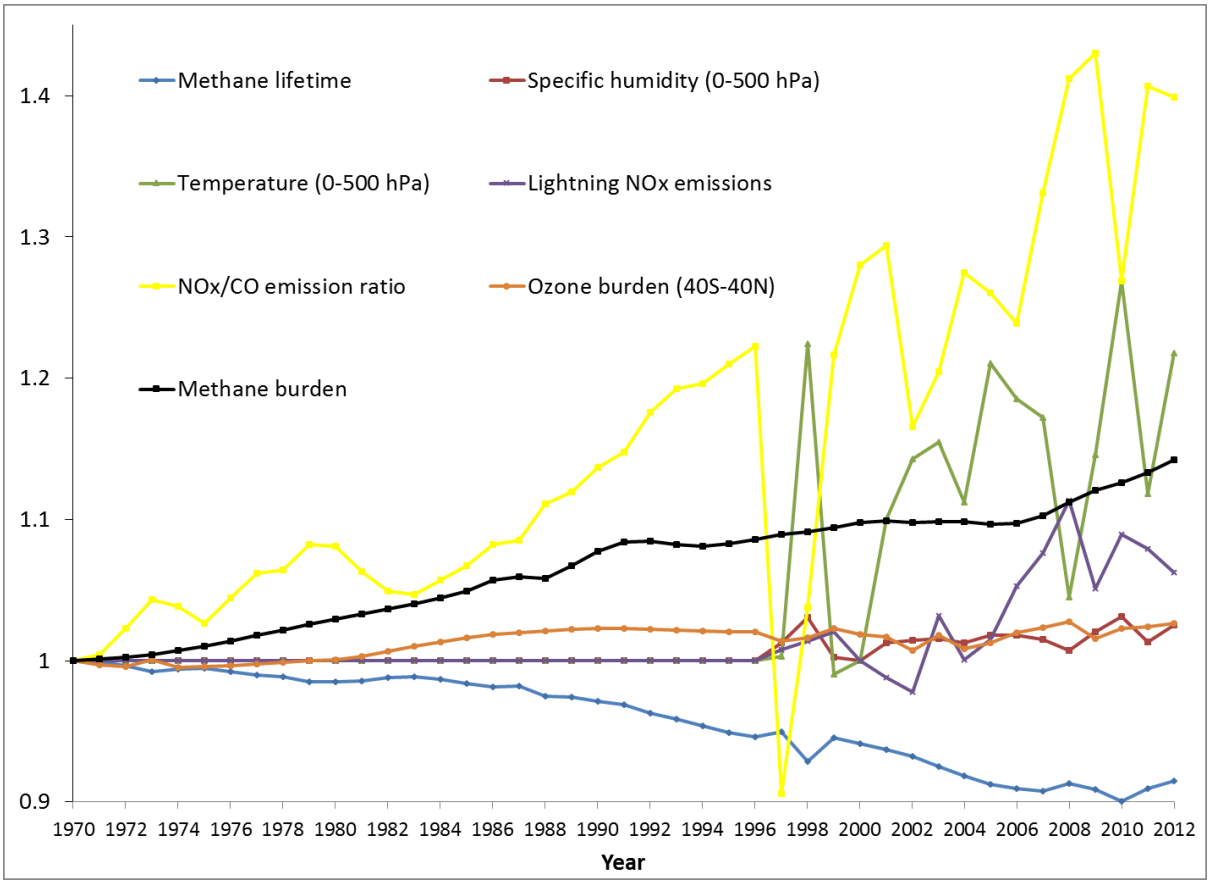

Figure 16. Development in atmospheric CH_4 lifetime and key parameters known to influence CH_4 lifetime. All variables values are relative to 1970. (To make it apparent in the figure temperature variations are relative to the Celsius scale).

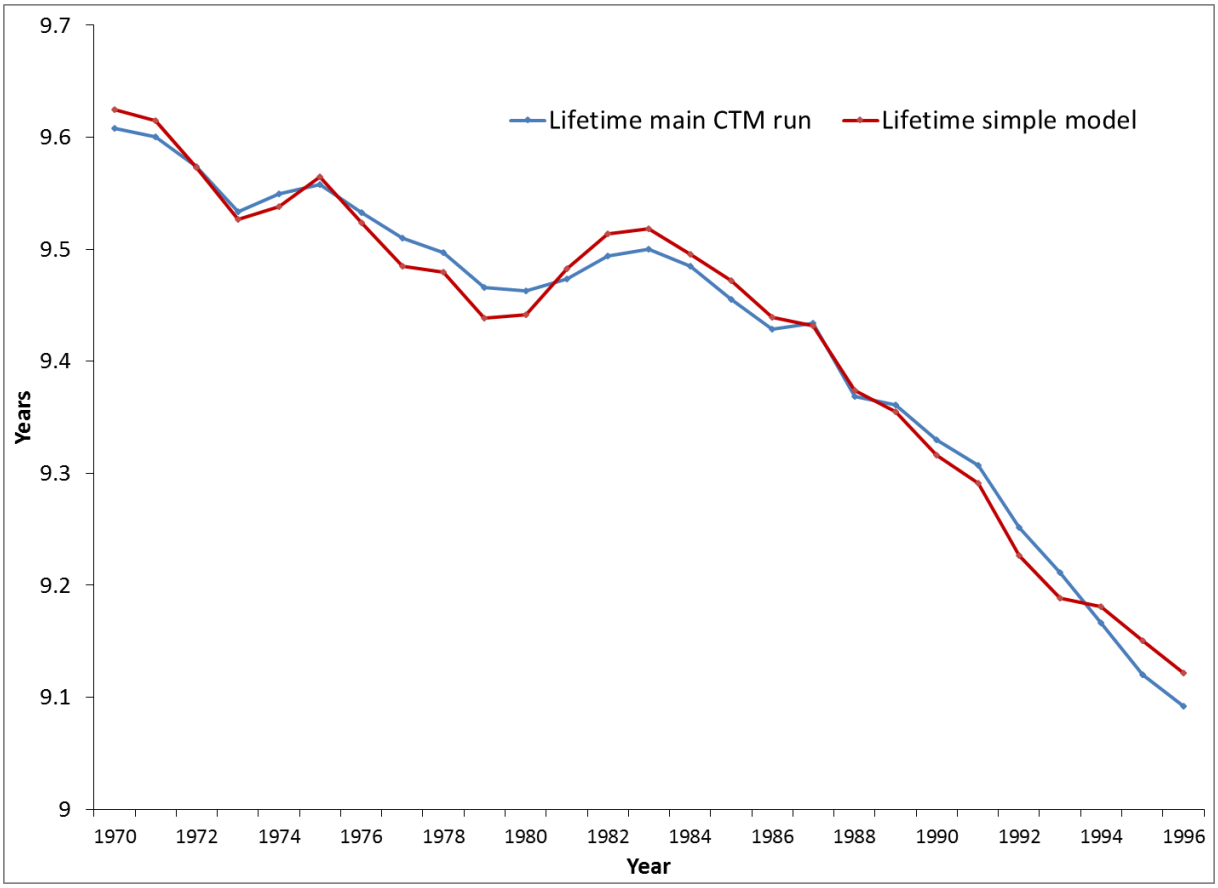

Figure 17. CH_4 lifetime evolution 1970-1996. Comparison of main model simulation (blue line) with CH_4 lifetime from simple model (red line) obtained from multiple linear regression.

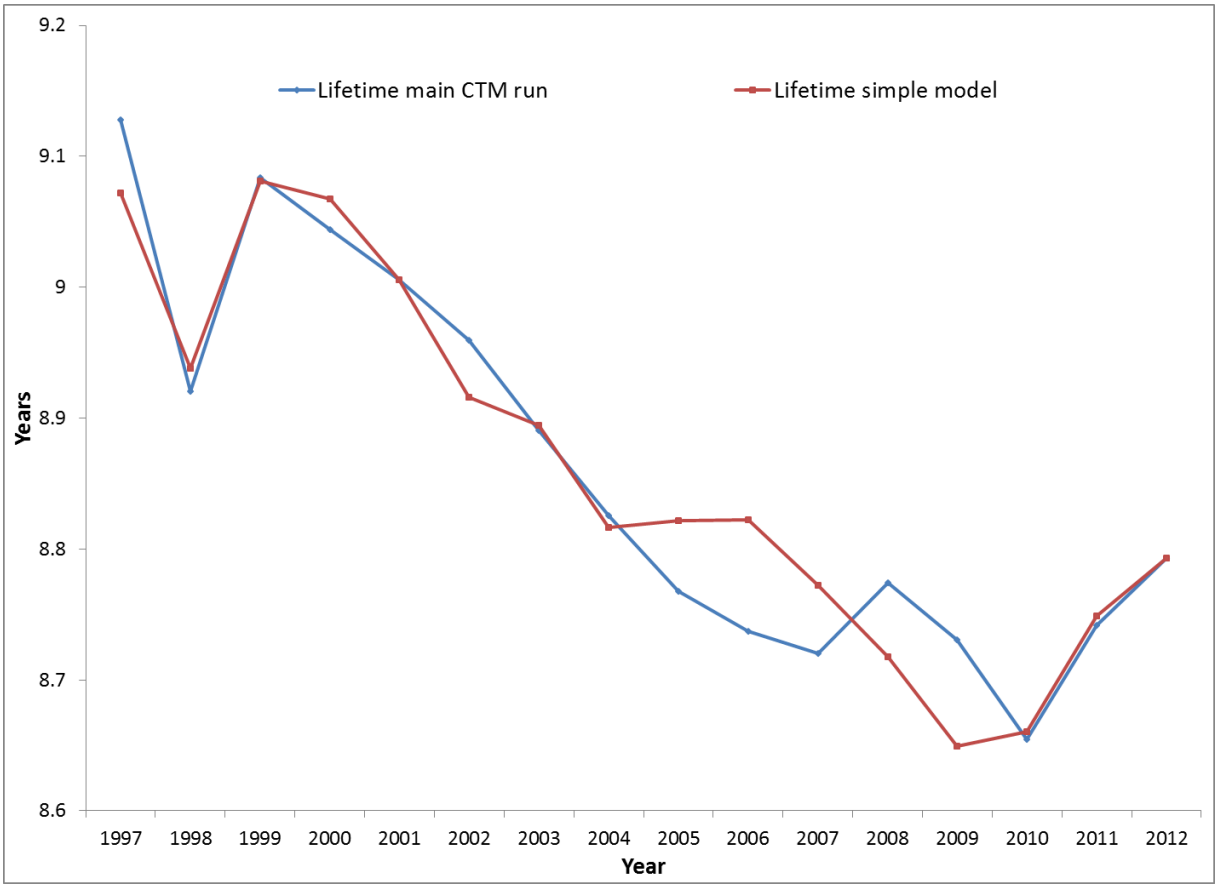

Figure 18. CH_4 lifetime evolution 1997-2012. Comparison of main model simulation (blue line) with CH_4 lifetime from simple model (red line) obtained from multiple linear regression.